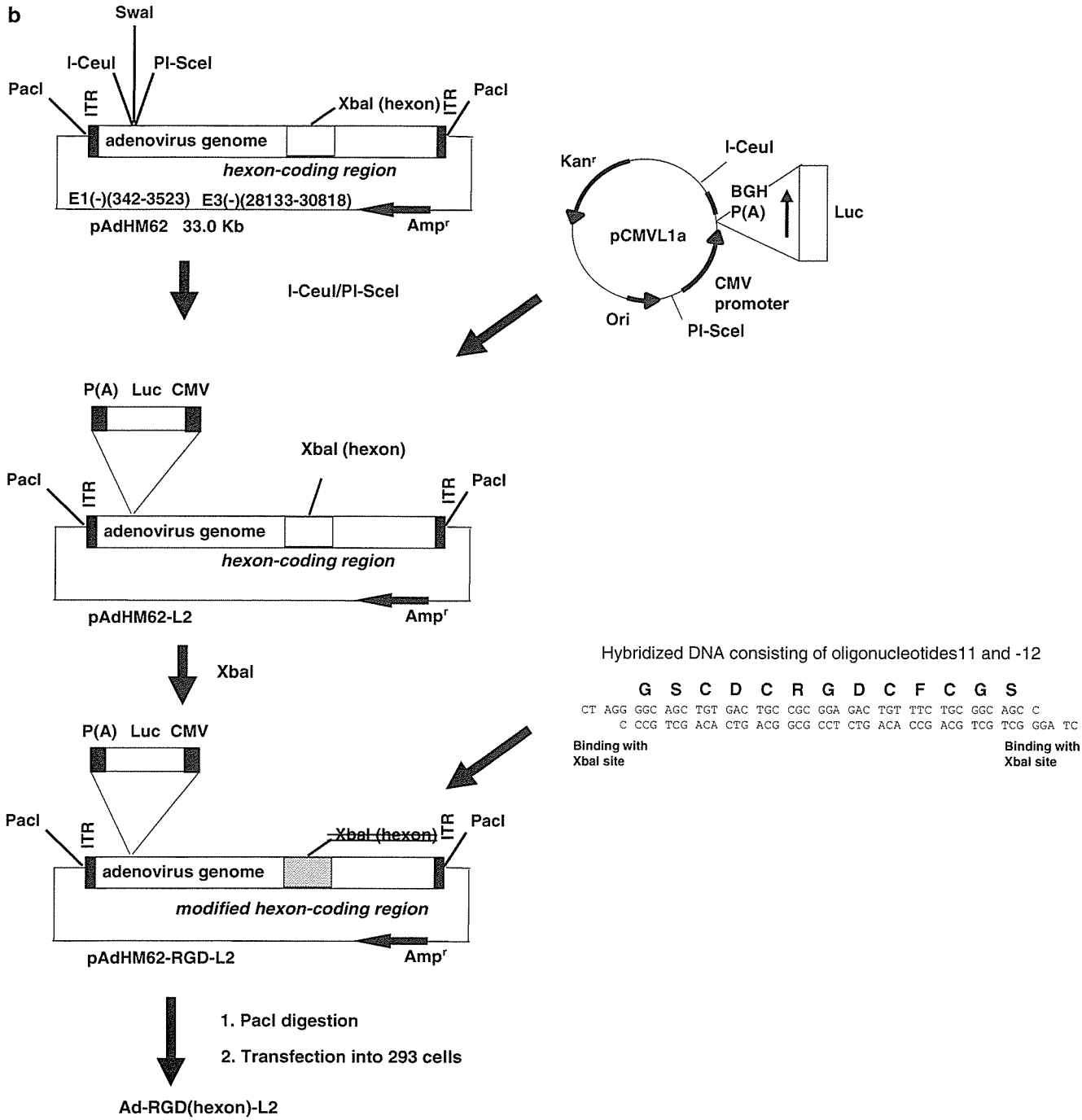

Figure 1 *Continued*

FLAG tag peptide in each region. Expression of the FLAG tag peptide in Ad-FLAG(HI)-L2, Ad-FLAG(C)-L2, Ad-FLAG(pIX)-L2 and Ad-FLAG(hexon)-L2 was examined by Western blotting. The total protein (1 μg) of each vector in 1 × sample buffer containing 4% β-mercaptoethanol was loaded on the SDS-PAGE gel after boiling 5 min, followed by electrotransfer to a PVDF (polyvinylidene difluoride) membrane. After blocking in Block Ace (Dainippon Pharmaceuticals, Osaka, Japan), the filters were incubated with ANTI-FLAG M2 monoclonal antibody (Sigma, Saint Louis, USA) (1:3000), followed by incubation in the presence of goat anti-mouse IgG HRP (Horseradish peroxidase)-linked antibody (Cell Signaling Technology Inc., MA, USA). The filters were developed by Chemi-Lumi One (Nacalai Tesque, Kyoto, Japan). The signals were read using a LAS-3000 machine (FUJIFILM, Tokyo, Japan). The FLAG tag peptide in the HI loop and the C-terminus of the fiber knob were about 60 kDa, similar size to a fiber protein. The molecular weight of pIX was 14.4 kDa and the FLAG tag peptide of Ad-FLAG(pIX)-L2 was about 14.4 kDa. The FLAG tag peptide detected in Ad-FLAG(hexon)-L2 was about 110 kDa, which is similar to the molecular weight of the hexon. Although the copy number of pIX is higher

Table 1 Oligonucleotides used in the present study

	Oligonucleotide	*Sequence of oligonucleotide (5′-3′)*
1	For 5′ region of 75 Å α-helical spacer (sense)	CTAGTTACAAGCTGGCCGACGAGGAGACGCGGGCACGGCTG TCCAAGGAGCTGCAGGCGGCGCAGGCCCGGCTGGGCGCGG ACATGGAGGACGTGTGC
2	For 5′ region of 75 Å α-helical spacer (antisense)	GGCCGCACACGTCCTCCATGTCCGCGCCCAGCCGGGCCTGC GCCGCCTGCAGCTCCTTGGACAGCCGTGCCCGCGTCTCCTC GTCGGCCAGCTTGTAA
3	For central region of 75 Å α-helical spacer (sense)	GGCCGCCTGGTGCAGTACCGCGGCGAGGTGCAGGCCATGCT CGGCCAGAGCACCGAGGAGCTGCGGGTGCGCCTCGCCTCCC ACCTGCGCAAGCTGCGTAAGCGGCTCG
4	For central region of 75 Å α-helical spacer (antisense)	TCGACGAGCCGCTTACGCAGCTTGCGCAGGTGGGAGGCGAG GCGCACCCGCAGCTCCTCGGTGCTCTGGCCGAGCATGGCCTG CACCTCGCCGCGGTACTGCACCAGGC
5	For 3′ region of 75 Å α-helical spacer (sense)	TCGAGATCCCAACCTATCTGAGCGAAGATGAACTGAAAGCC GCCGAAGCCGCCTTCAAACGCCACAACCCAACCGCGTTCGA AG
6	For 3′ region of 75 Å α-helical spacer (antisense)	GATCCTTCGAACGCGGTTGGGTTCTGGCGTTTGAAGGCGGCT TCGGCGGCTTTCAGTTCATCTTCGCTCAGATAGGTTGGGATC
7	For restriction enzyme sites from *Asc*I to *Xba*I at the downstream of 75 Å α-helical spacer of pHM15-75 A (sense)	AATTGGCGCGCCGCGGCCGCGTAAATGAATAGACTAGTGCTA GCCCTAGGTCTAGAGTGC
8	For restriction enzyme sites from *Asc*I to *Xba*I at the downstream of 75 Å α-helical spacer of pHM15-75 A (antisense)	TCTAGACCTAGGGCTAGCACTAGTCTATTCATTTACGCGGCCG CGGCGCGCC
9	For GS linker plus RGD-4C peptide into pHM15-75A (sense)	CGAGGGATCCGGTTCAGGGAGTGGCTCTTGTGACTGCCGCG GAGACTGTTTCTGCTAA
10	For GS linker plus RGD-4C peptide into pHM15-75A (antisense)	CGCGTTAGCAGAAACAGTCTCCGCGGCAGTCACAAGAGCCA CTCCCTGAACCGGATCCCT
11	For RGD-4C peptide into the C-terminus of pIX or HVR5 of hexon (sense)	CTAGGGGCAGCTGTGACTGCCGCGGAGACTGTTTCTGCGGCA GCC
12	For RGD-4C peptide into the C-terminus of pIX or HVR5 of hexon (antisense)	CTAGGGCTGCCGCAGAAACAGTCTCCGCGGCAGTCACAGCT GCCC
13	For FLAG tag sequence into the C-terminus of pIX or HVR5 of hexon (sense)	CTAGGGGCAGCGACTACAAGGACGATGATGACAAAGGCAG CC
14	For FLAG tag sequence into the C-terminus of pIX or HVR5 of hexon (antisense)	CTAGGGCTGCCTTTGTCATCATCGTCCTTGTAGTCGCTGCCC
15	For FLAG tag sequence into pHM15-75A (sense)	CGAGGGATCCGGTTCAGGGAGTGGCTCTGACTACAAGGACG ATGATGACAAATAA
16	For FLAG tag sequence into pHM15-75A (antisense)	CGCGTTATTTGTCATCATCGTCCTTGTAGTCAGAGCCACTCCC TGAACCGGATCCCT
17	For His tag sequence into the C-terminus of pIX (sense)	CTAGGGGCAGCCATCACCATCACCATCACGGCAGCC
18	For His tag sequence into the C-terminus of pIX (antisense)	CTAGGGCTGCCGTGATGGTGATGGTGATGGCTGCCC
19	For His tag sequence into pHM15-75A (sense)	CGAGGGATCCGGTTCAGGGAGTGGCTCTCATCACCATCACCA TCACTAA
20	For His tag sequence into pHM15-75A (antisense)	CGCGTTAGTGATGGTGATGGTGATGAGAGCCACTCCCTGAAC CGGATCCCT

than that of the fiber, the intensity of the band of Ad-FLAG(pIX)-L2 was weaker than that of Ad-FLAG(HI)-L2 and Ad-FLAG(C)-L2. This phenomenon is not due to impaired incorporation efficiency of the modified-pIX (at least the modified-pIX without the 75 Å α-helical spacer), because similar intensity of the pIX band was observed between Ad-FLAG(pIX)-L2 and Ad-L2 by Western blotting using anti-pIX antibody (kindly provided by Dr Keith N Leppard, Biological Sciences University of Warwick Coventry, UK)[27] (Figure 5b; will be described later). It remains unclear why the results of Figure 2 (anti-FLAG tag antibody) and Figure 5 (anti-pIX antibody) are different. The discrepancy might result from the property of each antibody. Anti-FLAG tag antibody is monoclonal, while anti-pIX antibody is polyclonal. These results suggested that the FLAG tag peptide was expressed as a fusion protein of the fiber, pIX or hexon.

Next, we examined by enzyme linked immunosorbent assay (ELISA) whether the FLAG tag peptide in each region was displayed on the virus surface (Figure 3). Purified viruses were incubated in carbonate-bicarbonate buffer (Sigma) and immobilized on a 96-well immunoplate (NALGE NUNC International, Tokyo, Japan) at 4°C. On the following day, wells were washed with phosphate buffered saline and blocked with Block Ace. Anti-FLAG tag monoclonal antibody (1:1000) diluted in Block Ace was bound to the immobilized virus and washed with phosphate-buffered saline containing 0.05% Tween20 (Polyxyethylene (20) Sorbitan Monolaurate; Wako Pure Chemical Industries Ltd, Osaka, Japan). Next, a secondary antibody (goat anti-mouse IgG HRP-linked antibody) diluted in Block Ace (1:1000) was bound to a mouse anti-FLAG tag antibody, and HRP was detected by TMB PEROXIDASE SUBSTRATE (MOSS Inc., Pasadena, ML, USA). Absorbance at 450–655 nm was measured by microplate reader. Ad-FLAG(HI)-L2, Ad-FLAG(C)-L2, Ad-FLAG(pIX)-L2 and Ad-FLAG(hexon)-L2 showed higher absorbance values than Ad-L2. Ad-FLAG(hexon)-L2 showed the highest absorbance values among all FLAG tag peptides displaying Ad vectors (Figure 3). The absorbance values were dependent on the copy number of the fusion protein on the

Table 2 Ad vectors used in the present study

Ad vectors	*Vector plasmids*	*Fiber*		*pIX*	*Hexon (HVR5)*
		HI loop	*C-terminus*		
Ad-L2	pAdHM4-L2	—	—	—	—
Ad-FLAG(HI)-L2	pAdHM41-FLAG(HI)-L2	DYKDDDDK	—	—	—
Ad-FLAG(C)-L2	pAdHM41-FLAG(C)-L2	—	$(GS)_4$DYKDDDDK	—	—
Ad-FLAG(pIX)-L2	pAdHM56-FLAG-L2	—	—	GSDYKDDDDKGS	—
Ad-FLAG(pIX/75)-L2	pAdHM56-FLAG75-L2	—	—	α-Helical linker plus $(GS)_4$DYKDDDDK	—
Ad-FLAG(hexon)-L2	pAdHM62-FLAG-L2	—	—	—	GSDYKDDDDKGS
Ad-His(pIX)-L2	pAdHM56-His-L2	—	—	GSHHHHHHGS	—
Ad-His(pIX/75)-L2	pAdHM56-His75-L2	—	—	α-Helical linker plus $(GS)_4$HHHHHH	—
Ad-RGD(HI)-L2	pAdHM15-RGD-L2	ACDCRGDCFCD	—	—	—
Ad-RGD(C)-L2	pAdHM41-RGD-L2	—	$(GS)_4$ACDCRGDCFCG	—	—
Ad-RGD(pIX)-L2	pAdHM56-RGD-L2	—	—	GSCDCRGDCFCGS	—
Ad-RGD(pIX/75)-L2	pAdHM56-RGD75-L2	—	—	α-helical linker plus $(GS)_4$CDCRGDCFC	—
Ad-RGD(hexon)-L2	pAdHM62-RGD-L2	—	—	—	GSCDCRGDCFCGS

Abbreviation: Ad, adenovirus.
Each modified Ad vector has additional amino-acids derived from unique restriction enzyme sites (*Csp*45I, *Cla*I or *Xba*I) in each region, but not be described here.

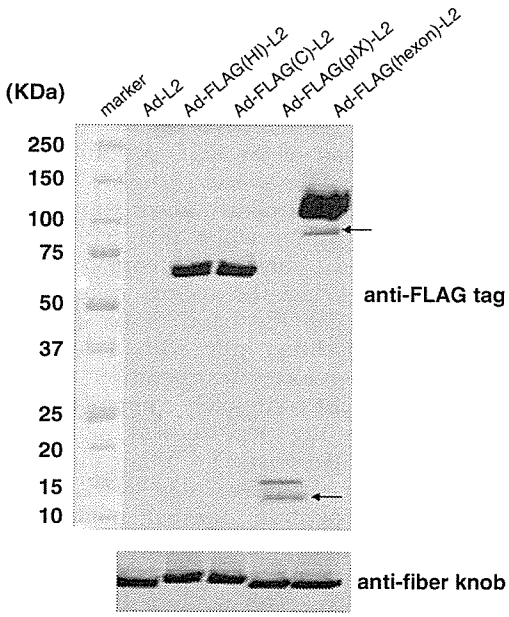

Figure 2 Western blotting of FLAG tag-modified Ad vectors. The total protein (1 μg) of each vector in 1 × sample buffer containing 4% β-mercaptoethanol was separated on a 4–20% SDS-PAGE gel, and the expression of the FLAG tag peptide was analyzed by Western blotting using mouse anti-FLAG tag monoclonal antibody. As a control, the membrane was also incubated with anti-fiber knob antibody (kindly provided by RD Gerard, University of Texas Southwestern Medical Center, Dallas, TX, USA). The band of the fiber of Ad-FLAG(HI)-L2 and Ad-FLAG(C)-L2 was higher than that of the other vectors, reflecting the insertion of the FLAG tag into the HI loop or C-terminus of the fiber knob. The extra bands marked with an arrow are proteolytic degradation products.

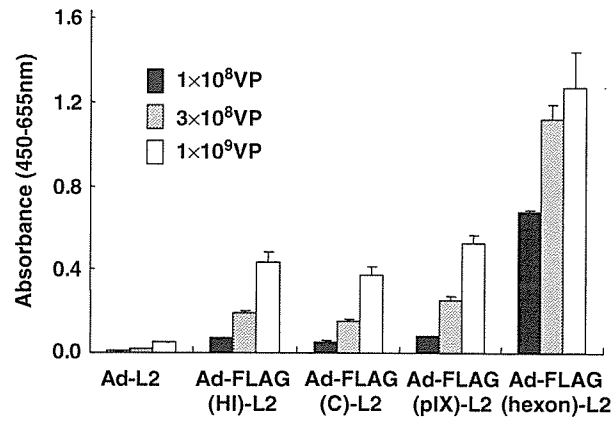

Figure 3 ELISA of FLAG tag-modified Ad vectors. Ad-L2, Ad-FLAG(HI)-L2, Ad-FLAG(C)-L2, Ad-FLAG(pIX)-L2 or Ad-FLAG(hexon)-L2 (10^9 VP/well, 3×10^8 VP/well, or 1×10^8 VP/well) were immobilized on a 96-well immunoplate. Mouse FLAG tag antibody was applied and then detected by anti-mouse IgG HRP-linked antibody. Absorbance at 450–655 nm was measured by microplate reader. The data are expressed as means ±s.d. ($n = 3$).

virus surface. Ad-FLAG(pIX)-L2, however, showed only slightly higher absorbance than Ad-FLAG(HI)-L2 and Ad-FLAG(C)-L2. ELISA is based on the ability of the anti-FLAG tag antibody to bind to the FLAG tag sequence on each Ad vector. The accessibility to the FLAG tag sequence at the C-terminus of pIX might be impaired, because pIX was buried between the hexon-tops. These results suggested that the fiber- (both the HI loop and C-terminus), pIX-, and the hexon-modified Ad vectors that were generated in this study did in fact display foreign ligands on the viral surface.

We and several groups have reported the feasibility of Ad vector application containing the RGD peptide in the HI loop or the C-terminus of the fiber knob, the C-terminus of pIX and the HVR5 region of the hexon.[9,10,18,21,28] However, there has been no report about which region is suitable for displaying the RGD peptide. To examine this, we constructed Ad vectors containing the RGD peptide in the fiber knob (HI loop or C-terminus), pIX (with or without 75 Å α-helical spacer),

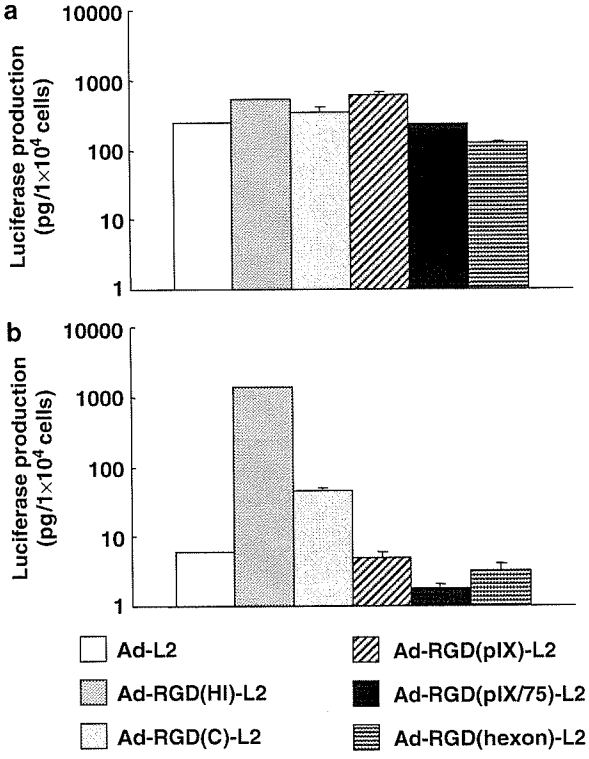

Figure 4 Transduction efficiency of RGD-modified Ad vectors. SK HEP-1 (**a**) and SF295 (**b**) cells were transduced with 3000 VP/cell of Ad-L2, Ad-RGD(HI)-L2, Ad-RGD(C)-L2, Ad-RGD(pIX)-L2, Ad-RGD(pIX/75A)-L2 or Ad-RGD(hexon)-L2 for 1.5 h, respectively. After culturing for 48 h, luciferase production was determined using a luciferase assay system (PicaGene LT2.0; Toyo Inki, Tokyo, Japan). The data are expressed as means ±s.d. ($n = 3$).

and hexon and compared the luciferase production in SK HEP-1 and SF295 cells transduced with each vector (Figure 4). In the case of the pIX-modified Ad vector, the vector containing the 75 Å α-helical spacer between the C-terminus of pIX and the RGD peptide was also constructed as described previously,[18] together with the vector without the α-helical spacer. The RGD (CDCRGDCFC; RGD-4C) peptide binds to integrin αvβ3 and αvβ5 on the cellular surface.[29–31] SK HEP-1 cells were CAR-positive, while SF295 cells were CAR-negative. Both cells expressed αvβ3 and αvβ5 integrins (the expression of CAR and integrins in each cell was examined in our previous report by flow cytometry).[28] The luciferase enzymatic activity following transduction with Ad-RGD(HI)-L2, Ad-RGD(C)-L2, Ad-RGD(pIX)-L2, Ad-RGD(pIX/75)-L2 and Ad-RGD(hexon)-L2 was only about two to three times different from that with Ad-L2 in SK HEP-1 cells (Figure 4a). This would reflect that all vectors efficiently transduce via (at least) CAR. In contrast, in SF295 cells Ad-RGD(HI)-L2 and Ad-RGD(C)-L2 showed approximately 230- or 10-fold higher luciferase production, which mediated via an RGD-integrin-dependent pathway (our previous data and data not shown),[10,28] than Ad-L2 (Figure 4b). Luciferase production in SF295 cells transduced with Ad-RGD(pIX)-L2, Ad-RGD(pIX/75)-L2 and Ad-RGD(hexon)-L2 were not enhanced compared with Ad-L2. Lower luciferase production in SF295 cells transduced with Ad-RGD(hexon)-L2 was due to the about four times lower ratio of infectious titer-to-particle titer of Ad-RGD(hexon)-L2 in comparison with that of Ad-L2. These results suggested that the HI loop of the fiber knob is the most suitable region for capsid modification at least in the case of the insertion of the RGD peptide.

Vellinga *et al.*[18] reported that Ad vectors containing the RGD peptide at the C-terminus of pIX with a 75 Å α-helical spacer could transduce more efficiently into CAR-negative Eoma cells than vectors with a 30 or 45 Å α-helical spacer or no spacer. In the present study, we used a similar α-helical spacer sequence to that used by Vellinga *et al.*,[18] but no enhanced transduction was observed. The level of gene expression of Ad-RGD(pIX/75)-L2 was approximately three times lower in the SF295 cells than Ad-L2. We speculated that the lower transduction efficiency of Ad-RGD(pIX/75)-L2 might be due to the decreased incorporation efficiency of pIX-spacer-RGD into Ad-RGD(pIX/75)-L2. Therefore, we examined the incorporation of pIX into virus particles by Western blotting using the anti-pIX antibody (Figure 5a). The data obtained suggested that the incorporation efficiency of pIX-spacer-RGD into Ad-RGD(pIX/75)-L2 was greatly decreased, and only a faint band (marked with an asterisk) was observed, while that of pIX-RGD into Ad-RGD(pIX)-L2 was similar to that into Ad-L2, a control virus (Figure 5a). Therefore, a longer spacer might hamper incorporation efficiency. This would be the reason why Ad-RGD(pIX/75)-L2 did not show increased transduction efficiency. To examine this phenomenon in more detail, the incorporation of modified-pIX with the FLAG tag or His tag (HHHHHH) peptide into each virus was examined instead of the RGD peptide (Figure 5b). Modified-pIX without the spacer (Ad-FLAG(pIX)-L2 and Ad-His(pIX)-L2) was similarly incorporated into the wild-type virus (Ad-L2), while that with the spacer (Ad-FLAG(pIX/75)-L2 and Ad-His(pIX/75)-L2) was severely impaired. When the vectors were over-loaded on the SDS-PAGE gel, the band of the RGD-, FLAG tag- or His tag-modified pIX with a longer spacer was observed. Therefore, incorporation efficiency of modified-pIX was not completely impaired (Figure 5c). The pIX-spacer-His tag peptide was more efficiently incorporated into Ad-His(pIX/75)-L2 than the pIX-spacer-FLAG into Ad-FLAG(pIX/75)-L2, suggesting that the kind of peptide inserted might affect the incorporation efficiency when the longer spacer sequence is used. Vellinga *et al.*[18] reported the generation of pIX-modified Ad vector with a longer spacer by co-transfection of vector plasmid lacking pIX coding region and the plasmid expresses a series of modified pIX. The incorporation efficiency of pIX with a longer spacer into virion was lower than that of conventional-pIX, although their efficiency was higher than that in the present study. Subtle differences in the linker sequence between pIX and the longer spacer or between the longer spacer and the RGD peptide might have caused this difference in results. Their group recently reported new method for generation of pIX-modified Ad vectors.[32] They created a series of helper cell lines producing modified-pIX with and without longer spacers. The incorporation efficiency of pIX with a longer spacer into virion generated by the method was similar to that of unmodified-pIX. They also showed that the heat-stability of pIX-modified Ad vector with a longer spacer was worse than that of the

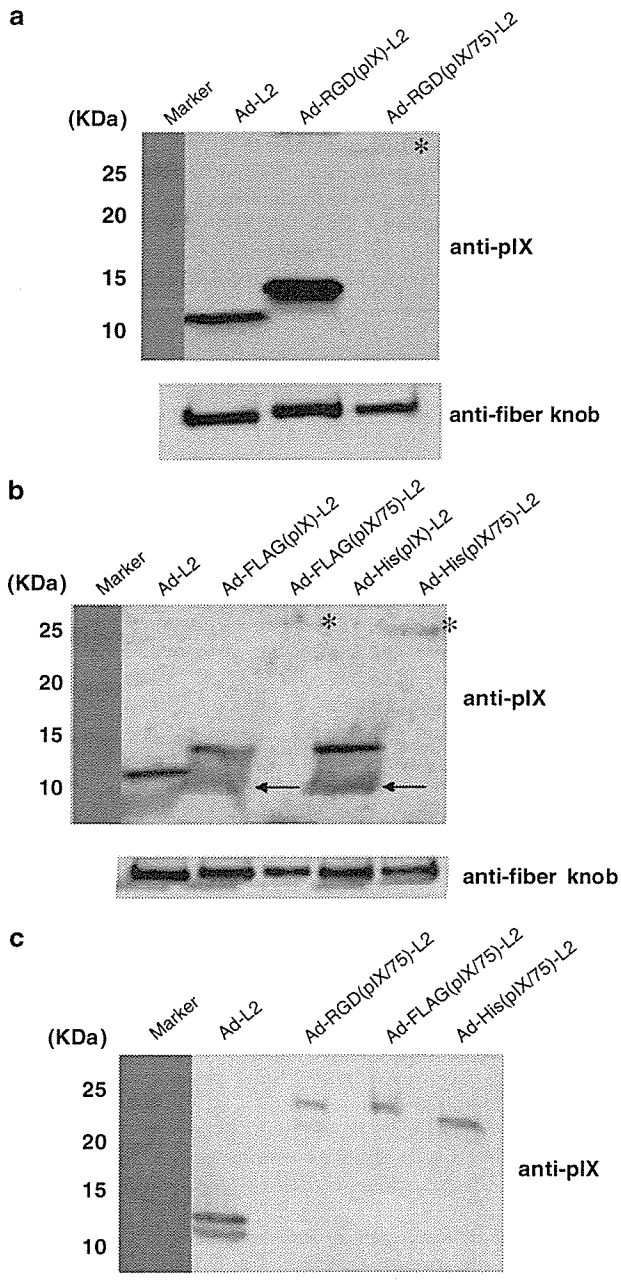

Figure 5 Analysis of the incorporation efficiency of modified-pIX. Incorporation efficiency of modified-pIX into the virus particles was determined by Western blotting. The total protein (**a** and **b**, 1 μg; **c**, 10 μg) of each vector in 1 × sample buffer containing 4% β-mercaptoethanol was separated on a 4–20% SDS-PAGE gel, and pIX was detected by the anti-pIX antibody. As a control, the anti-fiber knob antibody was used. (**a**) pIX-modified Ad vector containing the RGD peptide with or without a 75 Å α-helical spacer. (**b**) pIX-modified Ad vector containing the FLAG tag or His tag peptide with or without a 75 Å α-helical spacer. Ad-FLAG(pIX/75)-L2, Ad-His(pIX)-L2 and Ad-His(pIX/75)-L2 containing the FLAG tag or His tag peptide in the C-terminus of the pIX with or without a 75 Å α-helical spacer were similarly generated, as shown in Figure 1a. (**c**) The pIX-modifed Ad vector containing the RGD, FLAG tag, or His tag peptide with a 75 Å α-helical spacer. The extra bands marked with an arrow are proteolytic degradation products. The asterisks indicate the band of the modified-pIX with a 75 Å α-helical spacer.

conventional Ad vector and pIX-modified Ad vector without longer spacer. For these reasons, care should be taken in the use of a longer spacer.

Vigne *et al.*[21] have reported that Ad vectors containing the RGD peptide (DCRGDCF) at the HVR5 region of the hexon can infect cells via cellular αv integrin independently of CAR, which was inconsistent with the present study. The precise mechanism for these differences remains unclear. Subtle differences in the inserted RGD peptide sequence (SRGSCDCRGDCFCGSPR including the restriction enzyme-coding sequence in our study and GSDCRGDCFGS in their study) or the difference in the cell types used might have caused the discrepancy in results.

After we submitted this manuscript, Campos and Barry[33] reported a similar study in which fiber-, pIX- and hexon-modification were compared. They generated metabolically biotinylated Ad vectors by the insertion of the biotin acceptor peptide (BAP) in each location to directly compare targeted transduction through the fiber, pIX and hexon using a variety of biotinylated ligands, such as antibodies and proteins, which had a higher affinity than the RGD peptide. They reported that the modification of the fiber was more efficient than that of pIX and hexon,[33] which is consistent with the present report. They discussed how high affinity ligands at pIX or hexon made it impossible for the virus to escape from the endosome, and enter the cytoplasm, and traffic to the nucleus because the interaction between ligands at pIX or hexon and the cellular receptor was very strong. In the present study, we chose the RGD peptide to change (or expand) the tropism of the Ad vector, which had a lower affinity than antibodies or proteins. The modification of pIX and hexon with the RGD peptide might also have affected intracellular trafficking.

One of the possible reasons why the HI loop of the fiber knob is efficient in the case of the RGD peptide is that peptides displayed in the fiber knob can easily access the target molecules (receptors) because fiber knobs are the outmost capsid proteins of Ad vectors (the HI loop of the fiber knob is more exposed than the C-terminus). Therefore, pIX-modified or hexon-modified Ad vectors without the fiber proteins might show efficient ligand-mediated transduction because the ligand can come close to the cellular surface receptor. In addition, fiber-less Ad vectors do not infect cells via CAR due to the lack of fiber proteins.[34,35] pIX-modified or hexon-modified Ad vectors without fiber proteins could be a platform vector for targeting, although the fiber-less Ad vector was weaker against physical burdens, such as heat-treatment and freeze-and-thaw, than the conventional Ad vector (our unpublished data).

In summary, we have developed a simple method based on *in vitro* ligation to construct Ad vectors containing heterologous peptides in the C-terminus of pIX or the HVR5 region of the hexon. These Ad vectors displayed foreign peptides on the viral surface in each region. In the case of the insertion of the RGD peptide, Ad vectors modified in the HI loop of the fiber knob proved the better choice. As the vector system shown here enables easy construction of capsid-modified Ad vectors displaying a peptide of interest, it has great potential for gene therapy and gene transfer experiments.

Acknowledgements

The author thanks Tomomi Sasaki for technical assistance. This work was supported by grants from the

Ministry of Health, Labor, and Welfare of Japan. NK is the recipient of a fellowship from the Japan Society for the Promotion of Science.

References

1 Kovesdi I, Brough DE, Bruder JT, Wickham TJ. Adenoviral vectors for gene transfer. *Curr Opin Biotechnol* 1997; **8**: 583–589.
2 Benihoud K, Yeh P, Perricaudet M. Adenovirus vectors for gene delivery. *Curr Opin Biotechnol* 1999; **10**: 440–447.
3 Wickham TJ. Targeting adenovirus. *Gene Therapy* 2000; **7**: 110–114.
4 Mizuguchi H, Hayakawa T. Targeted adenovirus vectors. *Hum Gene Ther* 2004; **15**: 1034–1044.
5 Bergelson JM, Cunningham JA, Droguett G, Kurt-Jones EA, Krithivas A, Hong JS *et al*. Isolation of a common receptor for Coxsackie B viruses and adenoviruses 2 and 5. *Science* 1997; **275**: 1320–1323.
6 Tomko RP, Xu R, Philipson L. HCAR and MCAR: the human and mouse cellular receptors for subgroup C adenoviruses and group B coxsackieviruses. *Proc Natl Acad Sci USA* 1997; **94**: 3352–3356.
7 Dmitriev I, Krasnykh V, Miller CR, Wang M, Kashentseva E, Mikheeva G *et al*. An adenovirus vector with genetically modified fibers demonstrates expanded tropism via utilization of a coxsackievirus and adenovirus receptor-independent cell entry mechanism. *J Virol* 1998; **72**: 9706–9713.
8 Staba MJ, Wickham TJ, Kovesdi I, Hallahan DE. Modifications of the fiber in adenovirus vectors increase tropism for malignant glioma models. *Cancer Gene Ther* 2000; **7**: 13–19.
9 Mizuguchi H, Koizumi N, Hosono T, Utoguchi N, Watanabe Y, Kay MA *et al*. A simplified system for constructing recombinant adenoviral vectors containing heterologous peptides in the HI loop of their fiber knob. *Gene Therapy* 2001; **8**: 730–735.
10 Koizumi N, Mizuguchi H, Utoguchi N, Watanabe Y, Hayakawa T. Generation of fiber-modified adenovirus vectors containing heterologous peptides in both the HI loop and C terminus of the fiber knob. *J Gene Med* 2003; **5**: 267–276.
11 Dmitriev IP, Kashentseva EA, Curiel DT. Engineering of adenovirus vectors containing heterologous peptide sequences in the C terminus of capsid protein IX. *J Virol* 2002; **76**: 6893–6899.
12 Ghosh-Choudhury G, Haj-Ahmad Y, Graham FL. Protein IX, a minor component of the human adenovirus capsid, is essential for the packaging of full length genomes. *EMBO J* 1987; **6**: 1733–1739.
13 Furcinitti PS, van Oostrum J, Burnett RM. Adenovirus polypeptide IX revealed as capsid cement by difference images from electron microscopy and crystallography. *EMBO J* 1989; **8**: 3563–3570.
14 Rosa-Calatrava M, Grave L, Puvion-Dutilleul F, Chatton B, Kedinger C. Functional analysis of adenovirus protein IX identifies domains involved in capsid stability, transcriptional activity, and nuclear reorganization. *J Virol* 2001; **75**: 7131–7141.
15 Le LP, Everts M, Dmitriev IP, Davydova JG, Yamamoto M, Curiel DT. Fluorescently labeled adenovirus with pIX-EGFP for vector detection. *Mol Imag* 2004; **3**: 105–116.
16 Meulenbroek RA, Sargent KL, Lunde J, Jasmin BJ, Parks RJ. Use of adenovirus protein IX (pIX) to display large polypeptides on the virion–generation of fluorescent virus through the incorporation of pIX-GFP. *Mol Ther* 2004; **9**: 617–624.
17 Li J, Le L, Sibley DA, Mathis JM, Curiel DT. Genetic incorporation of HSV-1 thymidine kinase into the adenovirus protein IX for functional display on the virion. *Virology* 2005; **338**: 247–258.
18 Vellinga J, Rabelink MJ, Cramer SJ, van den Wollenberg DJ, Van der Meulen H, Leppard KN *et al*. Spacers increase the accessibility of peptide ligands linked to the carboxyl terminus of adenovirus minor capsid protein IX. *J Virol* 2004; **78**: 3470–3479.
19 Sumida SM, Truitt DM, Lemckert AA, Vogels R, Custers JH, Addo MM *et al*. Neutralizing antibodies to adenovirus serotype 5 vaccine vectors are directed primarily against the adenovirus hexon protein. *J Immunol* 2005; **174**: 7179–7185.
20 Roberts DM, Nanda A, Havenga MJ, Abbink P, Lynch DM, Ewald BA *et al*. Hexon-chimaeric adenovirus serotype 5 vectors circumvent pre-existing anti-vector immunity. *Nature* 2006; **441**: 239–243.
21 Vigne E, Mahfouz I, Dedieu JF, Brie A, Perricaudet M, Yeh P. RGD inclusion in the hexon monomer provides adenovirus type 5-based vectors with a fiber knob-independent pathway for infection. *J Virol* 1999; **73**: 5156–5161.
22 Wu H, Han T, Belousova N, Krasnykh V, Kashentseva E, Dmitriev I *et al*. Identification of sites in adenovirus hexon for foreign peptide incorporation. *J Virol* 2005; **79**: 3382–3390.
23 Mizuguchi H, Kay MA. A simple method for constructing E1- and E1/E4-deleted recombinant adenoviral vectors. *Hum Gene Ther* 1999; **10**: 2013–2017.
24 Mizuguchi H, Kay MA. Efficient construction of a recombinant adenovirus vector by an improved in vitro ligation method. *Hum Gene Ther* 1998; **9**: 2577–2583.
25 Mizuguchi H, Xu ZL, Sakurai F, Mayumi T, Hayakawa T. Tight positive regulation of transgene expression by a single adenovirus vector containing the rtTA and tTS expression cassettes in separate genome regions. *Hum Gene Ther* 2003; **14**: 1265–1277.
26 Maizel Jr JV, White DO, Scharff MD. The polypeptides of adenovirus. I. Evidence for multiple protein components in the virion and a comparison of types 2, 7A, and 12. *Virology* 1968; **36**: 115–125.
27 Caravokyri C, Leppard KN. Constitutive episomal expression of polypeptide IX (pIX) in a 293-based cell line complements the deficiency of pIX mutant adenovirus type 5. *J Virol* 1995; **69**: 6627–6633.
28 Koizumi N, Mizuguchi H, Hosono T, Ishii-Watabe A, Uchida E, Utoguchi N *et al*. Efficient gene transfer by fiber-mutant adenoviral vectors containing RGD peptide. *Biochim Biophys Acta* 2001; **1568**: 13–20.
29 Koivunen E, Wang B, Ruoslahti E. Phage libraries displaying cyclic peptides with different ring sizes: ligand specificities of the RGD-directed integrins. *Biotechnology (New York)* 1995; **13**: 265–270.
30 Pasqualini R, Koivunen E, Ruoslahti E. Alpha v integrins as receptors for tumor targeting by circulating ligands. *Nat Biotechnol* 1997; **15**: 542–546.
31 Arap W, Pasqualini R, Ruoslahti E. Cancer treatment by targeted drug delivery to tumor vasculature in a mouse model. *Science* 1998; **279**: 377–380.
32 Vellinga J, Uil TG, de Vrij J, Rabelink MJ, Lindholm L, Hoeben RC. A system for efficient generation of adenovirus protein IX-producing helper cell lines. *J Gene Med* 2006; **8**: 147–154.
33 Campos SK, Barry MA. Comparison of adenovirus fiber, protein IX, and hexon capsomeres as scaffolds for vector purification and cell targeting. *Virology* 2006; **349**: 453–462.
34 Legrand V, Spehner D, Schlesinger Y, Settelen N, Pavirani A, Mehtali M. Fiberless recombinant adenoviruses: virus maturation and infectivity in the absence of fiber. *J Virol* 1999; **73**: 907–919.
35 Von Seggern DJ, Chiu CY, Fleck SK, Stewart PL, Nemerow GR. A helper-independent adenovirus vector with E1, E3, and fiber deleted: structure and infectivity of fiberless particles. *J Virol* 1999; **73**: 1601–1608.

HUMAN GENE THERAPY 18:74–80 (January 2007)

DOI: 10.1089/hum.2006.129

Technical Report

Rapid Construction of Small Interfering RNA-Expressing Adenoviral Vectors on the Basis of Direct Cloning of Short Hairpin RNA-Coding DNAs

HIROYUKI MIZUGUCHI,[1,2] NAOKO FUNAKOSHI,[1] TETSUJI HOSONO,[3] FUMINORI SAKURAI,[1] KENJI KAWABATA,[1] TERUHIDE YAMAGUCHI,[3] and TAKAO HAYAKAWA[4]

ABSTRACT

In the conventional method for constructing an adenoviral (Ad) vector expressing small interfering RNA (siRNA), short hairpin RNA (shRNA)-coding oligonucleotides are introduced downstream of a polymerase III (or polymerase II)-based promoter cloned into a shuttle plasmid. An siRNA expression cassette, which is cloned into the shuttle plasmid, is then introduced into the E1 deletion region of the Ad vector plasmid by *in vitro* ligation or homologous recombination in *Escherichia coli*, and the linearized plasmid is transfected into 293 cells, generating an Ad vector expressing siRNA. Therefore, two-step plasmid manipulation is required. In this study, we developed a method by which shRNA-coding oligonucleotides can be introduced directly into the Ad vector plasmid. To do this, we constructed a new vector plasmid into which the human U6 promoter sequence was cloned in advance. Unique restriction enzyme sites were introduced at the transcription start site of the U6 promoter sequence in the vector plasmid. Luciferase and p53 genes were efficiently knocked down by Ad vectors generated by the new method and expressing siRNA against the target gene. This method should be useful for RNA interference-based experiments, and should make it easy to construct an siRNA-expressing Ad vector library for functional screening.

INTRODUCTION

RNA INTERFERENCE (RNAi), which mediates the sequence-specific suppression of gene expression in a wide variety of eukaryotes by double-stranded RNA homologies to the target gene (Scherer and Rossi, 2003), is a powerful tool for the knockdown of gene expression. Transduction of synthetic small interfering RNA (siRNA; 19 to 29 nucleotides of RNA) or the promoter-based expression of siRNA in the cells results in sequence-dependent degradation of target mRNA and subsequent reduction of target gene expression. Most promoter-based RNAi systems express short hairpin RNA (shRNA), which is then trimmed by Dicer, generating functional siRNA. Polymerase III-based promoters, such as the small nuclear RNA U6 promoter or the human RNase P RNA H1 promoter, are widely used for the expression of shRNA (siRNA) (Scherer and Rossi, 2003), although polymerase II-based promoters are also used (Xia *et al.*, 2002; Shinagawa and Ishii, 2003). The promoter-based method has an advantage in that viral vectors as well as nonviral vectors can be used for delivery of the siRNA expression unit, whereas only nonviral vectors are used for delivery of synthetic siRNA.

Recombinant adenoviral (Ad) vectors have been used extensively to deliver foreign genes to a variety of cell types and tissues both *in vitro* and *in vivo* (McConnell and Imperiale, 2004; Volpers and Kochanek, 2004). They can be easily grown to high titers and can efficiently transfer genes into both dividing and nondividing cells. Therefore, Ad vector-mediated

[1]National Institute of Biomedical Innovation, Osaka 567-0085, Japan.
[2]Graduate School of Pharmaceutical Sciences, Osaka University, Osaka 567-0871, Japan.
[3]National Institute of Health Sciences, Tokyo 158-8501, Japan.
[4]Pharmaceuticals and Medical Devices Agency, Tokyo 100-0013, Japan.

delivery of an siRNA expression unit, in which a promoter-based shRNA expression cassette is delivered into the cell by the Ad vector, provides a valuable tool for both gene function studies and therapeutic applications.

Construction of Ad vectors used to be a time-consuming and labor-intensive procedure, but several improved methods to facilitate the construction of Ad vectors have been developed (reviewed in Mizuguchi *et al.*, 2001). The homologous recombination method in E1-complementing cell lines (i.e., 293 cells) has been the most widely used method for generating recombinant Ad vectors, and it has greatly contributed to the widespread use of Ad vectors (Bett *et al.*, 1994). The major limitations of this approach are the low frequency of the recombination event and the tedious and time-consuming plaque purification procedure required to select the recombinant virus of interest, because a relatively high percentage of the virus produced is wild type (in most cases, 20–70%), due to recombination with the Ad sequence integrated into the chromosomes of 293 cells. The improved *in vitro* ligation method (Mizuguchi and Kay, 1998, 1999) and the homologous recombination method in *Escherichia coli* (He *et al.*, 1998), which are commercially available from Clontech (Palo Alto, CA) and Invitrogen (Carlsbad, CA), respectively, have now become widely used, because these systems overcome the limitations of the homologous recombination method in 293 cells. To construct an Ad vector expressing siRNA by these two methods, shRNA-coding oligonucleotides are introduced downstream of the polymerase III (or polymerase II)-based promoter cloned in a shuttle plasmid. An shRNA (siRNA) expression cassette, which is cloned in the shuttle plasmid, is then introduced into the E1 deletion region of the Ad vector plasmid, which clones a full Ad genome, by simple *in vitro* ligation or homologous recombination in *E. coli*. The resulting plasmid is then linearized and transfected into 293 cells, generating an Ad vector expressing siRNA. Therefore, two-step *E. coli* transformation and plasmid manipulation is required for the improved *in vitro* ligation method, whereas three-step *E. coli* transformation and plasmid manipulation is required in the homologous recombination method in *E. coli* (because a special *E. coli* strain is used in the latter method, retransformation into a normal stain of *E. coli* is required) (reviewed in Mizuguchi *et al.*, 2001).

In the present study, we developed a simple method for generating an Ad vector expressing siRNA, in which shRNA-coding oligonucleotides could be directly introduced into an Ad vector plasmid containing the human U6 (hU6) promoter sequence. Unique restriction enzyme sites were introduced at the transcription start site of the hU6 promoter sequence cloned into the Ad vector plasmid. Two types of modified hU6 promoter sequence were constructed to develop this method. Using this method, only one-step *E. coli* transformation is required to generate an Ad vector plasmid containing an siRNA expression cassette.

MATERIALS AND METHODS

Cells

A549 and 293 cells were cultured in Dulbecco's modified Eagle's medium (DMEM) supplemented with 10% fetal calf serum (FCS). A549-Luc cells, which are stable transformants with luciferase expression, were cultured in DMEM supplemented with 10% FCS. For construction of A549-Luc cells, A549 cells were transfected with luciferase-expressing plasmid pGL3-Control-RSVneo, which contains the simian virus 40 (SV40) promoter/enhancer-luciferase cDNA-SV40 p(A) sequence and the neomycin expression cassette, using SuperFect transfection reagent (Qiagen, Valencia, CA). pGL3-Control-RSVneo was constructed by insertion of the Rous sarcoma virus (RSV) promoter-driven neomycin expression cassette into pGL3-Control (Promega, Madison, WI). Monoclonal A549 cells stably expressing luciferase (A549-Luc) were obtained by geneticin (G418) selection.

Plasmid and virus

The hU6 promoter sequence was amplified from human genomic DNA (Clontech), using the following primers: hU6-S1, hU6-AS1, and hU6-AS2 (Table 1). The hU6a and hU6b promoter sequences were amplified with hU6-S1/hU6-AS1 and hU6-S1/hU6-AS2 primer sets, respectively (see Fig. 2). These promoter sequences were introduced into pHM5 (Mizuguchi and Kay, 1999), and were then transferred into the E1 deletion region of the vector plasmid pAdHM4.1, a derivative of pAdHM4 (Mizuguchi and Kay, 1998) (the *Xba*I site outside the Ad genome of pAdHM4 was deleted), by an *in vitro* ligation method using the I-*Ceu*I and PI-*Sce*I sites (Mizuguchi and Kay, 1998, 1999), resulting in pAdHM4-hU6a and pAdHM4-hU6b, respectively (Fig. 1A). To construct a vector plasmid containing an shRNA-coding sequence against luciferase, oligonucleotides 1/2 and 3/4 were synthesized (Table 1), annealed, and cloned into the *Cla*I and *Xba*I sites of pAdHM4-hU6a or the *Swa*I and *Xba*I sites of pAdHM4-hU6b, generating pAdHM4-hU6a-Lu and pAdHM4-hU6b-Lu, respectively. The target sequence for siRNA is bp 158 to 176 of luciferase cDNA. For the construction of vector plasmid containing shRNA-coding sequence against p53 (Brummelkamp *et al.*, 2002), oligonucleotides 5/6 and 7/8 were used for cloning into the *Cla*I and *Xba*I sites of pAdHM4-hU6a or the *Swa*I and *Xba*I sites of pAdHM4-hU6b, generating pAdHM4-hU6a-p53 and pAdHM4-hU6b-p53, respectively. The target sequence for siRNA is bp 775 to 793 of human p53 cDNA.

The original intact hU6 promoter sequence, derived from an *Eco*RI/*Sal*I fragment of piGene hU6 (iGENE Therapeutics, Tsukuba, Japan), was also introduced into the *Sph*I and *Sal*I sites of pHM5 (Mizuguchi and Kay, 1999), resulting in pHM5-ihU6. pHM5-ihU6 was then digested with *Sal*I and *Xba*I, and ligated with oligonucleotides 9 and 10, resulting in pHM5-hU6. In this case, oligonucleotides 11/12 and 13/14 (for the shRNA-coding sequence against luciferase and p53, respectively) were introduced into the *Bsp*MI site of pHM5-hU6 according to the report of Miyagishi *et al.* (2004) and the manufacturer's instructions (iGENE Therapeutics); and then an siRNA expression cassette was inserted into the E1-deletion region of pAdHM4 (Mizuguchi and Kay, 1998), using the I-*Ceu*I and PI-*Sce*I sites, resulting in pAdHM4-hU6-Lu and pAdHM4-hU6-p53, respectively. The sequence was verified with a DNA sequencer (ABI PRISM 310; Applied Biosystems, Foster City, CA).

Viruses (Ad-hU6-Lu, Ad-hU6a-Lu, Ad-hU6b-Lu, Ad-hU6-p53, Ad-hU6a-p53, and Ad-hU6b-p53) were prepared by the

TABLE 1. OLIGONUCLEOTIDES USED IN THE PRESENT STUDY

Oligonucleotide	*Sequence of oligonucleotide (5′–3′)*
hU6-S1 primer	aaggtcgggcaggaagagggccta
hU6-AS1 primer	ggtctagaagt*atcgat*tttcgtctttccacaagatatat (*Xba*I and *Cla*I recognition sequences are underlined and italicized, respectively)
hU6-AS2 primer	ggtctagaagt*atttaaat*tcgtcctttccacaagatatataa (*Xba*I and *Swa*I recognition sequences are underlined and italicized, respectively)
Oligonucleotide 1	cg*acgctgagtacttcgaaat*ttcaagaga*atttcgaagtactcagcgt*tttttggaaat (loop sequences and siRNA-coding sequence are underlined and italicized, respectively)
Oligonucleotide 2	ctagatttccaaaaa*acgctgagtacttcgaaat*tctcttgaa*atttcgaagtactcagcgt* (loop sequences and siRNA-coding sequence are underlined and italicized, respectively)
Oligonucleotide 3	cc*acgctgagtacttcgaaat*ttcaagaga*atttcgaagtactcagcgt*tttttggaaat (loop sequences and siRNA-coding sequence are underlined and italicized, respectively)
Oligonucleotide 4	ctagatttccaaaaa*acgctgagtacttcgaaat*tctcttgaa*atttcgaagtactcagcgtgg* (loop sequences and siRNA-coding sequence are underlined and italicized, respectively)
Oligonucleotide 5	cg*gactccagtggtaatctac*ttcaagaga*gtagattaccactggagtc*tttttggaaat (loop sequences and siRNA-coding sequence are underlined and italicized, respectively)
Oligonucleotide 6	ctagatttccaaaaa*gactccagtggtaatctac*tctcttgaa*gtagattaccactggagtc* (loop sequences and siRNA-coding sequence are underlined and italicized, respectively)
Oligonucleotide 7	cc*gactccagtggtaatctac*ttcaagaga*gtagattaccactggagtc*tttttggaaat (loop sequences and siRNA-coding sequence are underlined and italicized, respectively)
Oligonucleotide 8	ctagatttccaaaaa*gactccagtggtaatctac*tctcttgaa*gtagattaccactggagtc*gg (loop sequences and siRNA-coding sequence are underlined and italicized, respectively)
Oligonucleotide 9	tcgacctgcaggcatgcaagcttc (BspMI recognition sequences are underlined)
Oligonucleotide 10	ctaggaagcttgcatgcctgcagg (BspMI recognition sequences are underlined)
Oligonucleotide 11	cacc*acgctgagtacttcgaaat*ttcaagaga*atttcgaagtactcagcgt*ttttt (loop sequences and siRNA-coding sequence are underlined and italicized, respectively)
Oligonucleotide 12	gcataaaaa*acgctgagtacttcgaaat*tctcttgaa*atttcgaagtactcagcgt* (loop sequences and siRNA-coding sequence are underlined and italicized, respectively)
Oligonucleotide 13	cacc*gactccagtggtaatctac*ttcaagaga*gtagattaccactggagtc*tttttt (loop sequences and siRNA-coding sequence are underlined and italicized, respectively)
Oligonucleotide 14	gcataaaaa*gactccagtggtaatctac*tctcttgaa*gtagattaccactggagtc* (loop sequences and siRNA-coding sequence are underlined and italicized, respectively)

transfection of a *Pac*I-linearized vector plasmid (pAdHM4-hU6-Lu, pAdHM4-hU6a-Lu, pAdHM4-hU6b-Lu, pAdHM4-hU6-p53, pAdHM4-hU6a-p53, and pAdHM4-hU6b-p53, respectively) into 293 cells as described previously (Mizuguchi and Kay, 1998). Ad vectors containing only the original intact hU6 promoter sequence (without a target sequence; Ad-hU6) were similarly constructed with pHM5-hU6 and pAdHM4. The virus was purified by $CsCl_2$ gradient centrifugation; dialyzed with a solution containing 10 m*M* Tris (pH 7.5), 1 m*M* $MgCl_2$, and 10% glycerol; and stored in aliquots at −70°C. Determination of virus particle (VP) titers and infectious titers was accomplished spectrophotometrically by the method of Maizel *et al.* (1968) and with an Adeno-X rapid titer kit (Clontech), respectively. The infectious titer-to-particle ratio was 1:36 for Ad-hU6, 1:31 for Ad-hU6-Lu, 1:28 for Ad-hU6a-Lu, 1:24 for Ad-hU6b-Lu, 1:22 for Ad-hU6-p53, 1:12 for Ad-hU6a-p53, and 1:15 for Ad-hU6b-p53.

Adenovirus-mediated gene transduction and luciferase assay

A549 cells (2×10^5 cells) were seeded into a 12-well dish. The next day, they were transduced with the Ad vectors for 1.5 hr. Determination of luciferase production in the cells and extraction of cellular protein for Western blotting were performed after a 72-hr culture period. Luciferase production in the cells was measured with a luciferase assay system (PicaGene LT 2.0; produced by Toyo Ink [Tokyo, Japan] for Wako [Kyoto, Japan])

Western blotting for p53

Cell extracts were prepared in lysis buffer (25 m*M* Tris [pH 7.5], 1% Triton X-100, 0.5% sodium deoxycholate, 5 m*M* EDTA, 150 m*M* NaCl) containing a cocktail of protease inhibitors (Sigma, St. Louis, MO). The protein content was measured

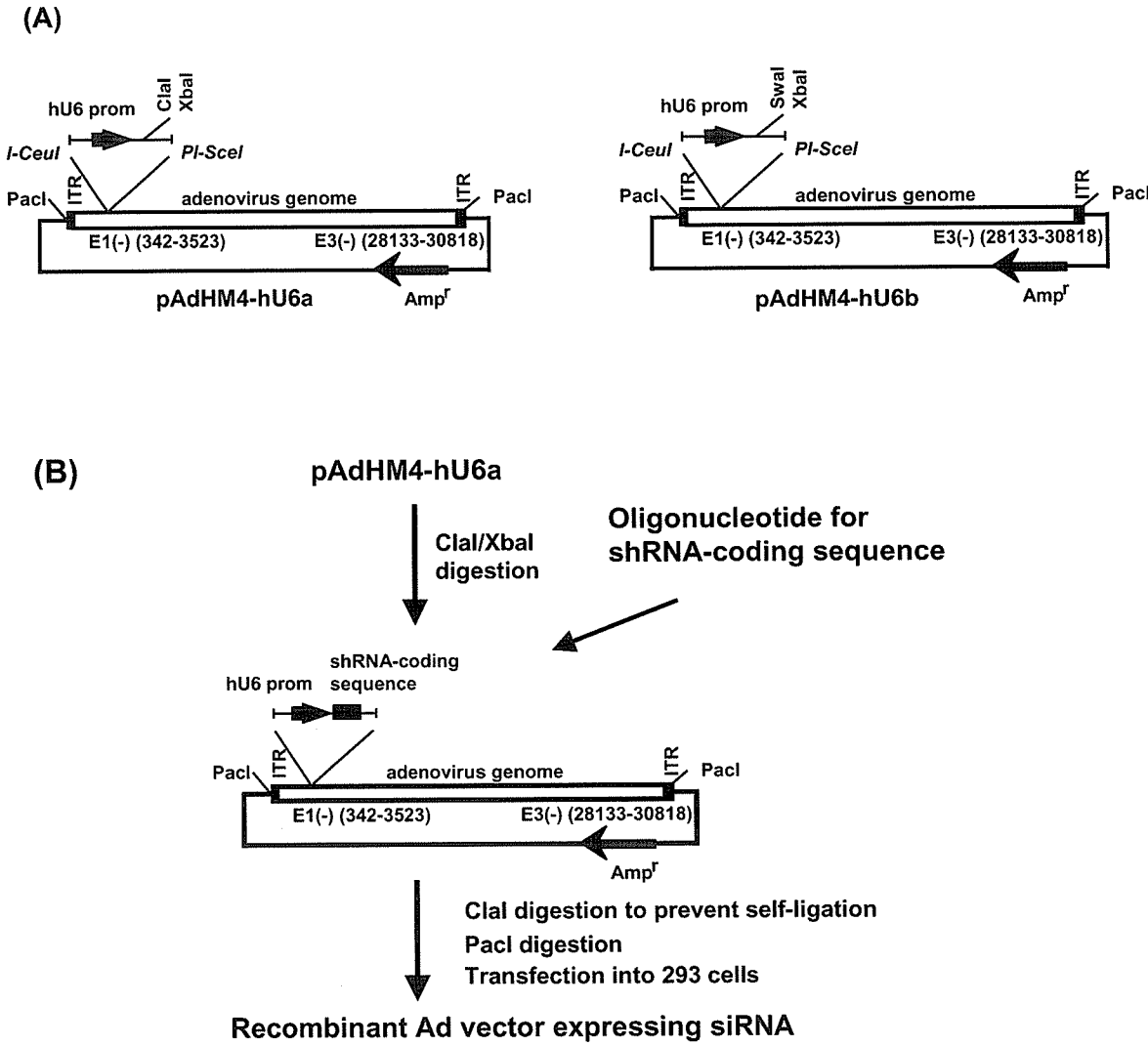

FIG. 1. Vector plasmids and the construction strategy for Ad vectors expressing siRNA. (**A**) Vector plasmids pAdHM4-hU6a and pAdHM4-hU6b. pAdHM4-hU6a contains a unique *Cla*I site at the transcription start site of the hU6 promoter sequence and an *Xba*I site downstream from the promoter sequence. pAdHM4-hU6b contains a unique *Swa*I site at the transcription start site of the hU6 promoter sequence and an *Xba*I site downstream from the promoter sequence. (**B**) Construction strategy for the Ad vector expressing siRNA. pAdHM4-hU6a was digested with *Cla*I/*Xba*I and ligated with oligonucleotides for the shRNA-coding sequence. Ligation products were then digested with *Cla*I to prevent the generation of nonrecombinant parental plasmid. The resulting plasmid was linearized by digestion with *Pac*I and transfected into 293 cells, generating recombinant Ad vectors expressing siRNA. pAdHM4-hU6b was similarly used.

with a Bio-Rad assay kit (Bio-Rad, Hercules, CA), using bovine serum albumin as the standard. Protein samples (10 μg) were electrophoresed on sodium dodecyl sulfate (SDS)– 12.5% polyacrylamide gels under reducing conditions, followed by electrotransfer to Immobilon-P membranes (Millipore, Bedford, MA). After blocking in nonfat dry milk, the filters were incubated with antibodies against p53 (Santa Cruz Biotechnology, Santa Cruz, CA) and actin (Oncogene Research Products/EMD Biosciences, San Diego, CA), followed by incubation in the presence of peroxidase-labeled goat anti-mouse IgG antibody (American Qualex Antibodies, San Clemente, CA) or peroxidase-labeled goat anti-mouse IgM antibody (Oncogene Research Products/EMD Biosciences). The filters were developed by chemiluminescence (ECL Western blotting detection system; GE Healthcare, Piscataway, NJ). The signals were read with an LAS-3000 (Fujifilm, Tokyo, Japan), and quantified with Image Gauge software (Fujifilm).

RESULTS AND DISCUSSION

Rapid and efficient construction of Ad vectors expressing siRNA offers the promise of using RNAi in the context of both gene function analysis and therapeutic applications. In the present study, we developed a simple method for constructing Ad vectors expressing siRNA, based on only one-step *in vitro* ligation. To do this, we first constructed an Ad vector plasmid containing the E1- and E3-deleted Ad genome and the hU6 pro-

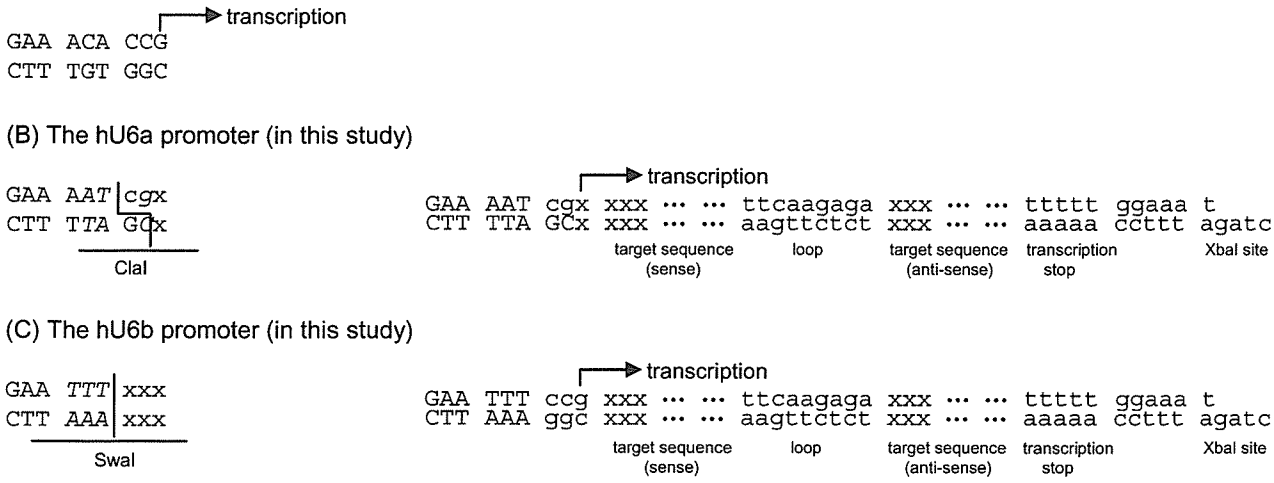

FIG. 2. Sequences at the transcription start site of the new hU6 promoter. (**A**) Intact hU6 promoter sequence. (**B**) hU6a promoter sequence. In this promoter, the *Cla*I site is placed at the transcription start site. (**C**) hU6b promoter sequence. In this promoter, a *Swa*I site is placed at the transcription start site. shRNA-coding oligonucleotides to be synthesized for each promoter are shown as lower-case letters on the right-hand side.

moter sequence in the E1 deletion region, pAdHM4-hU6a and pAdHM4-hU6b (Fig. 1A). By introducing the hU6 promoter sequence into the vector plasmid in advance, the cloning step of the gene of interest from the shuttle plasmid to the vector plasmid, which is an essential step in the conventional method for constructing Ad vectors (namely, the improved *in vitro* ligation method [Mizuguchi and Kay, 1998, 1999] and homologous recombination method in *E. coli* [He *et al.*, 1998]), can be skipped. To make it possible to directly clone the shRNA-coding oligonucleotides downstream of the hU6 promoter sequence, hU6 promoters containing unique restriction enzyme sites at the transcription start site have been developed. The new hU6 promoter sequences contain a *Cla*I or *Swa*I site around the transcription start site and an *Xba*I site downstream from the promoter (Figs. 1 and 2). These enzyme sites were selected because they do not cut the E1- and E3-deleted Ad genome. Because the transcription of shRNA might be influenced by the mutated sequences around the transcription start site, two types of hU6 promoters, differing by only a few nucleotides, were constructed. The hU6a promoter sequence contains a *Cla*I site, whereas the hU6b promoter sequence contains a *Swa*I site. *Cla*I, *Swa*I, and *Xba*I sites are unique in the vector plasmids pAdHM4-hU6a and pAdHM4-hU6b. To generate a recombinant vector plasmid for Ad vectors expressing siRNA, oligonucleotides for shRNA against the target gene were synthesized, annealed, and ligated with *Cla*I/*Xba*I-digested pAdHM4-hU6a or *Swa*I/*Xba*I-digested pAdHM4-hU6b. Oligonucleotides were designed so that recombinant vector plasmid containing the shRNA-coding sequence is redigested with *Xba*I, but not with *Cla*I or *Swa*I. By designing oligonucleotides like the one described above, the generation of self-ligated plasmid can be avoided by digestion of the ligation products with *Cla*I or *Swa*I. On the right side of Fig. 2, DNA sequences, including the shRNA-coding sequence around the transcription start site of the hU6 promoter, are shown. Oligonucleotides that must be synthesized for the shRNA-coding sequence are shown as lower-case letters. By using the method developed in the present study, we could easily generate Ad vectors expressing siRNAs against luciferase and human p53. More than 90% of the recombinant Ad vector plasmids contained the correct insert. Because the *Cla*I- (or *Swa*I-) and *Xba*I-digested pAdHM4-hU6a and pAdHM4-hU6b can be stored at −20°C, only the ligation-based introduction of oligonucleotides into these sites of the vector plasmid would be required for the construction of an appropriate vector.

To examine the function of Ad vectors expressing siRNA against luciferase (Ad-hU6a-Lu and Ad-hU6b-Lu), the efficiency of knockdown of luciferase expression in A549-Luc cells, which stably express luciferase, was examined by treatment with Ad-hU6a-Lu or Ad-hU6b-Lu (Fig. 3). Ad-hU6-Lu, in which the hU6 promoter contains the original intact sequence even after introduction of an shRNA-coding sequence, was used as a positive control. To generate Ad-hU6-Lu, the shRNA-coding sequence was first introduced downstream from the hU6 promoter sequence cloned into the shuttle plasmid, according to the report of Miyagishi *et al.* (2004) and the manufacturer's instructions (iGENE Therapeutics); the shRNA expression cassette was then introduced into the E1 deletion region of the Ad vector plasmid pAdHM4 (Mizuguchi and Kay, 1998). Transfection of a *Pac*I-digested vector plasmid into 293 cells generated Ad-hU6-Lu. Ad-hU6, which contains the intact hU6 promoter without the shRNA-coding sequence, and Ad-hU6-p53, which contains the intact hU6 promoter with the shRNA-coding sequence against human p53, were similarly constructed and used as negative controls. Data showed that Ad-hU6a-Lu and Ad-hU6b-Lu suppressed luciferase expression in A549-Luc cells as efficiently as Ad-hU6-Lu, in a dose-dependent manner (Fig. 3). Ad-hU6 and Ad-hU6-p53 showed no effects on luciferase expression. Ad-hU6a-p53 and Ad-hU6b-p53 (these Ad vectors are used in Fig. 4) also had no influence on luciferase expression (data not shown). The RNAi effect of luciferase expression was relatively weak compared with that of p53 (de-

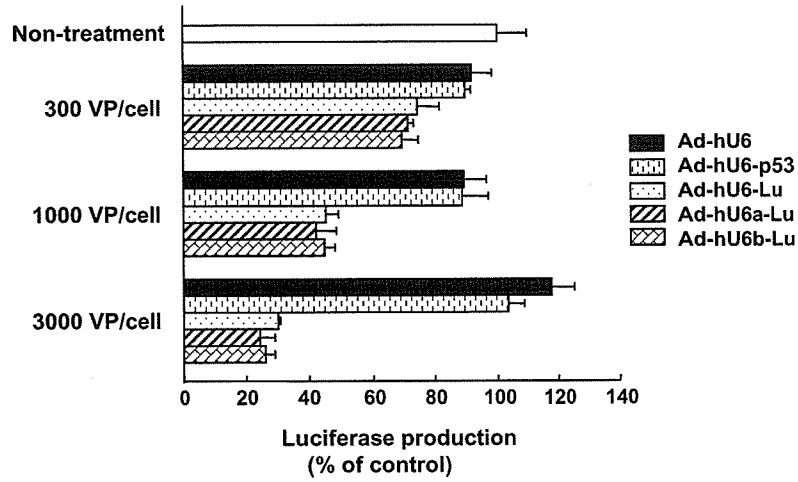

FIG. 3. Suppression of luciferase expression by Ad vector expressing siRNA. A549-Luc cells, which stably express luciferase, were transduced for 1.5 hr with Ad-hU6, Ad-hU6-p53, Ad-hU6-Lu, Ad-hU6a-Lu, or Ad-hU6b-Lu at 300, 1000, or 3000 VP/cell. After culturing for 72 hr, luciferase production in the cells was measured by luminescence assay. Data are expressed as means and SD ($n = 4$).

scribed below). This difference probably occurred because the A549-Luc cells were expressing luciferase from a strong viral promoter (SV40 promoter and enhancer) and because the levels of luciferase expression were higher than those of endogenous p53 expression.

We next examined the RNAi effect of the siRNA-expressing Ad vector generated in the present study on the endogenous gene. As a model, we silenced p53 expression in A549 cells (Fig. 4). Ad-hU6a-p53 and Ad-hU6b-p53 were generated, and Ad-hU6, Ad-hU6-Lu, and Ad-hU6-p53 were also used. Ad-hU6-p53 contains the intact hU6 promoter sequence, including the transcription start site, even after introduction of the shRNA-coding sequence. A549 cells were transduced with a 300- or 1000-VP/cell of each Ad vector, and cultured for 3 days. Levels of p53 expression were examined by Western blotting. Expression of actin was also measured as an internal control. Expression of p53 in A549 cells was efficiently decreased by treatment with Ad-hU6a-p53 and Ad-hU6b-p53 as well as with Ad-hU6-p53. Levels of p53 expression in cells treated with Ad-hU6-p53, Ad-hU6a-p53, or Ad-hU6b-p53 at 1000 VP/cell were decreased to 7, 2, and 5%, respectively, relative to cells treated with Ad-hU6, according to Image Gauge software (Fujifilm) (in the case of 300 VP/cell, they were decreased to 53, 24, and 30%, respectively). The efficiency of p53 silencing by treatment with Ad-hU6-p53 was slightly lower than that with Ad-hU6a-p53 or Ad-hU6b-p53. This reduced efficiency is likely due to the approximately 1.5 to 2 times lower infectious titer-to-particle titer ratio of Ad-hU6-p53 in comparison with those of Ad-hU6a-p53 and Ad-hU6b-p53. Ad-hU6 and Ad-hU6-Lu did not decrease the level of p53 expression (Fig. 4). These results indicate that new hU6 promoters containing *Cla*I or *Swa*I sites at the transcription start site should transcribe as efficiently as the original hU6 promoter, and that Ad vectors containing the new hU6 promoters efficiently silence target gene expression. Different vector systems (pAdHM4-hU6a and pAdHM4-hU6b) should be used according to the specific purpose.

To facilitate the construction of an siRNA expression plasmid, the U6 and H1 promoters, which contain *Apa*I, *Bbs*I, *Bgl*II, *Eco*RV, *Sal*I, and *Xba*I sites, etc., at the transcription start site, have been developed (Brummelkamp *et al.*, 2002; Lee *et al.*, 2002; Paddison *et al.*, 2002; Paul *et al.*, 2002; Sui *et al.*, 2002; Yu *et al.*, 2002; Boden *et al.*, 2003). All types of promoters worked efficiently, and could be widely used for efficient RNAi, although the efficiency (activity) of the mutated promoters described above has not been compared with that of the intact promoter. The present study clearly showed that the mutated hU6 promoter, at least one having a *Cla*I or *Swa*I site at the transcription start site and an *Xba*I site downstream of the promoter sequence, is similar in activity to the intact hU6 promoter and would not influence the function of the promoter.

The method using polymerase chain reaction (PCR)-based amplification of shRNA together with the U6 promoter followed by subsequent cloning of the complete expression cassette directly into the Ad vector genome is another strategy for one-step construction of recombinant Ad plasmids containing an siRNA expression cassette. In this method, however, the procedures described below are required for preparation of insert DNA: (1) ordering of the PCR primer, (2) PCR, (3) purification of the PCR product, (4) restriction enzyme digestion and purification of the PCR product, and (5) ligation. In our present system, only the following procedures are required: (1) ordering of the oligonucleotides, (2) hybridization of the oligonucleotides, and (3) ligation. Thus, the present method would be much easier and would allow any laboratory to easily construct

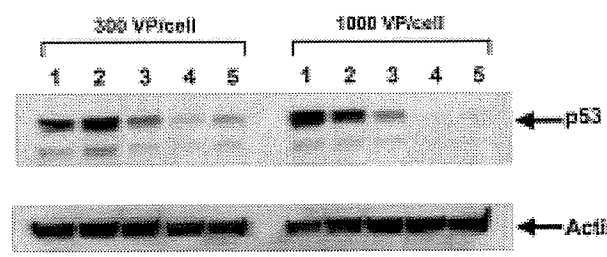

FIG. 4. Suppression of human p53 expression by Ad vector expressing siRNA. A549 cells were transduced for 1.5 hr with Ad-hU6 (lane 1), Ad-hU6-Lu (lane 2), Ad-hU6-p53 (lane 3), Ad-hU6a-p53 (lane 4), or Ad-hU6b-p53 (lane 5) at 300 or 1000 VP/cell, and then cultured for 3 days. Proteins were then extracted from the cells, and the levels of p53 expression were examined by Western blotting. The actin bands served as an internal control for equal total protein loading. The extra (lower) bands of p53 are nonspecific.

Ad vectors expressing siRNA for gene transfer studies and therapeutic applications.

Various types of promoters that are based on polymerase II as well as polymerase III have been developed to transcribe shRNA (siRNA) (Xia *et al.*, 2002; Shinagawa and Ishii, 2003). Although the present study applied the most commonly used U6 promoter for simple and efficient construction of siRNA-expressing Ad vectors, this method could easily be applied to vectors using other promoters including polymerase II-based promoters. This method can also easily be combined with various types of improved Ad vectors, such as Ad vectors containing capsid modification (Koizumi *et al.*, 2003, 2006; Mizuguchi and Hayakawa, 2004; Kurachi *et al.*, 2006) or Ad vectors belonging to different subgroups to modify tropism (Sakurai *et al.*, 2003), and Ad vectors containing a tetracycline-inducible RNAi system (Hosono *et al.*, 2004). The method developed in the present study should be a powerful tool for the application of RNAi, and might facilitate the development of an siRNA-expressing Ad vector library for functional screening.

ACKNOWLEDGMENTS

The authors thank Risako Nagahashi-Nakano and Tomomi Sasaki for technical assistance. This work was supported by grants from the Ministry of Health, Labor, and Welfare of Japan.

REFERENCES

BETT, A.J., HADDARA, W., PREVEC, L., and GRAHAM, F.L. (1994). An efficient and flexible system for construction of adenovirus vectors with insertions or deletions in early regions 1 and 3. Proc. Natl. Acad. Sci. U.S.A. **91,** 8802–8806.

BODEN, D., PUSCH, O., LEE, F., TUCKER, L., SHANK, P.R., and RAMRATNAM, B. (2003). Promoter choice affects the potency of HIV-1 specific RNA interference. Nucleic Acids Res. **31,** 5033–5038.

BRUMMELKAMP, T.R., BERNARDS, R., and AGAMI, R. (2002). A system for stable expression of short interfering RNAs in mammalian cells. Science **296,** 550–553.

HE, T.C., ZHOU, S., DA COSTA, L.T., YU, J., KINZLER, K.W., and VOGELSTEIN, B. (1998). A simplified system for generating recombinant adenoviruses. Proc. Natl. Acad. Sci. U.S.A. **95,** 2509–2514.

HOSONO, T., MIZUGUCHI, H., KATAYAMA, K., XU, Z.L., SAKURAI, F., ISHII-WATABE, A., KAWABATA, K., YAMAGUCHI, T., NAKAGAWA, S., MAYUMI, T., and HAYAKAWA, T. (2004). Adenovirus vector-mediated doxycycline-inducible RNA interference. Hum. Gene Ther. **15,** 813–819.

KOIZUMI, N., MIZUGUCHI, H., UTOGUCHI, N., WATANABE, Y., and HAYAKAWA, T. (2003). Generation of fiber-modified adenovirus vectors containing heterologous peptides in both the HI loop and C terminus of the fiber knob. J. Gene Med. **5,** 267–276.

KOIZUMI, N., KAWABATA, K., SAKURAI, F., WATANABE, Y., HAYAKAWA, T., and MIZUGUCHI, H. (2006). Modified adenoviral vectors ablated for coxsackievirus–adenovirus receptor, α_v integrin, and heparan sulfate binding reduce *in vivo* tissue transduction and toxicity. Hum. Gene Ther. **17,** 264–279.

KURACHI, S., KOIZUMI, N., SAKURAI, F., KAWABATA, K., SAKURAI, H., NAKAGAWA, S., HAYAKAWA, T. and MIZUGUCHI, H. (2006). Characterization of capsid-modified adenovirus vectors containing heterologous peptides in the fiber knob, protein IX, or hexon. Gene Ther. (in press).

LEE, N.S., DOHJIMA, T., BAUER, G., LI, H., LI, M.J., EHSANI, A., SALVATERRA, P., and ROSSI, J. (2002). Expression of small interfering RNAs targeted against HIV-1 *rev* transcripts in human cells. Nat. Biotechnol. **20,** 500–505.

MAIZEL, J.V., Jr., WHITE, D.O., and SCHARFF, M.D. (1968). The polypeptides of adenovirus. I. Evidence for multiple protein components in the virion and a comparison of types 2, 7A, and 12. Virology **36,** 115–125.

McCONNELL, M.J., and IMPERIALE, M.J. (2004). Biology of adenovirus and its use as a vector for gene therapy. Hum. Gene Ther. **15,** 1022–1033.

MIYAGISHI, M., SUMIMOTO, H., MIYOSHI, H., KAWAKAMI, Y., and TAIRA, K. (2004). Optimization of an siRNA-expression system with an improved hairpin and its significant suppressive effects in mammalian cells. J. Gene Med. **6,** 715–723.

MIZUGUCHI, H., and HAYAKAWA, T. (2004). Targeted adenovirus vectors. Hum. Gene Ther. **15,** 1034–1044.

MIZUGUCHI, H., and KAY, M.A. (1998). Efficient construction of a recombinant adenovirus vector by an improved *in vitro* ligation method. Hum. Gene Ther. **9,** 2577–2583.

MIZUGUCHI, H., and KAY, M.A. (1999). A simple method for constructing E1- and E1/E4-deleted recombinant adenoviral vectors. Hum. Gene Ther. **10,** 2013–2017.

MIZUGUCHI, H., KAY, M.A., and HAYAKAWA, T. (2001). Approaches for generating recombinant adenovirus vectors. Adv. Drug Deliv. Rev. **52,** 165–176.

PADDISON, P.J., CAUDY, A.A., BERNSTEIN, E., HANNON, G.J., and CONKLIN, D.S. (2002). Short hairpin RNAs (shRNAs) induce sequence-specific silencing in mammalian cells. Genes Dev. **16,** 948–958.

PAUL, C.P., GOOD, P.D., WINER, I., and ENGELKE, D.R. (2002). Effective expression of small interfering RNA in human cells. Nat. Biotechnol. **20,** 505–508.

SAKURAI, F., MIZUGUCHI, H., and HAYAKAWA, T. (2003). Efficient gene transfer into human $CD34^+$ cells by an adenovirus type 35 vector. Gene Ther. **10,** 1041–1048.

SCHERER, L.J., and ROSSI, J.J. (2003). Approaches for the sequence-specific knockdown of mRNA. Nat. Biotechnol. **21,** 1457–1465.

SHINAGAWA, T., and ISHII, S. (2003). Generation of Ski-knockdown mice by expressing a long double-strand RNA from an RNA polymerase II promoter. Genes Dev. **17,** 1340–1345.

SUI, G., SOOHOO, C., AFFAR EL, B., GAY, F., SHI, Y., and FORRESTER, W.C. (2002). A DNA vector-based RNAi technology to suppress gene expression in mammalian cells. Proc. Natl. Acad. Sci. U.S.A. **99,** 5515–5520.

VOLPERS, C., and KOCHANEK, S. (2004). Adenoviral vectors for gene transfer and therapy. J. Gene Med. **6,** S164–S171.

XIA, H., MAO, Q., PAULSON, H.L., and DAVIDSON, B.L. (2002). siRNA-mediated gene silencing *in vitro* and *in vivo*. Nat. Biotechnol. **20,** 1006–1010.

YU, J.Y., DERUITER, S.L., and TURNER, D.L. (2002). RNA interference by expression of short-interfering RNAs and hairpin RNAs in mammalian cells. Proc. Natl. Acad. Sci. U.S.A. **99,** 6047–6052.

Address reprint requests to:
Dr. Hiroyuki Mizuguchi
National Institute of Biomedical Innovation
Asagi 7-6-8, Saito
Ibaraki, Osaka 567-0085, Japan

E-mail: mizuguch@nibio.go.jp

Received for publication September 3, 2006; accepted after revision November 12, 2006.

Published online: December 22, 2006.

BIOCHEMICAL PHARMACOLOGY 73 (2007) 206–214

available at www.sciencedirect.com

ScienceDirect

journal homepage: www.elsevier.com/locate/biochempharm

Role of tyrosine residues in modulation of claudin-4 by the C-terminal fragment of *Clostridium perfringens* enterotoxin

Motoki Harada [a,1], *Masuo Kondoh* [b,1,*], *Chiaki Ebihara* [a], *Azusa Takahashi* [a], *Eriko Komiya* [a], *Makiko Fujii* [a], *Hiroyuki Mizuguchi* [c,d], *Shin-Ichi Tsunoda* [e], *Yasuhiko Horiguchi* [f], *Kiyohito Yagi* [b], *Yoshiteru Watanabe* [a]

[a] *Department of Pharmaceutics and Biopharmaceutics, Showa Pharmaceutical University, Machida, Tokyo 194-8543, Japan*
[b] *Department of Bio-Functional Molecular Chemistry, Graduate School of Pharmaceutical Sciences, Osaka University, Suita, Osaka 565-0871, Japan*
[c] *Laboratory of Gene Transfer and Regulation, National Institute of Biomedical Innovation, Ibaraki, Osaka 567-0085, Japan*
[d] *Graduate School of Pharmaceutical Sciences, Osaka University, Suita, Osaka 565-0871, Japan*
[e] *Laboratory of Pharmaceutical Proteomics, National Institute of Biomedical Innovation, Ibaraki, Osaka 567-0085, Japan*
[f] *Department of Bacterial and Toxinology, Division of Infectious Diseases, Osaka University, Suita, Osaka 565-0871, Japan*

ARTICLE INFO

Article history:
Received 21 August 2006
Accepted 3 October 2006

Keywords:
Claudin-4
Clostridium perfringens enterotoxin
Caco-2 cells
Tight junction
Barrier-function

ABSTRACT

The C-terminal fragment of *Clostridium perfringens* enterotoxin (C-CPE) modulates the barrier function of claudin-4 via its C-terminal 16 amino acids. In the current study, we investigated the roles of tyrosine residues (Y306, Y310 and Y312) in this region in the modulation of TJs by C-CPE. Single mutations of Y306, Y310 and Y312 to alanine resulted in partial reduction of claudin-4 binding. We also prepared double mutants of C-CPE to further evaluate the roles of these tyrosine residues. Replacement of Y310 and Y312 with alanine (Y310A/Y312A) partly reduced the ability of C-CPE to bind to claudin-4. Double mutants Y306A/Y310A and Y306A/Y312A, however, lost the ability to bind to claudin-4 and to modulate the TJ barrier. We also found that a triple mutant (Y306A/Y310A/Y312A) lost the ability to bind claudin-4, modulate the TJ barrier, and enhance jejunal absorption in rats. These results indicate that tyrosines 306, 310, and 312 are critical for the interaction of C-CPE with claudin-4 and for the modulation of TJ barrier function by C-CPE. This study provides information that should help in the development of claudin modulators based on C-CPE.

1. Introduction

Tight junctions (TJs) play a central role in sealing the intercellular space in epithelial and endothelial sheets [1,2]. The key structure in this regard is the TJ strand, which lies within the plasma membrane. Each TJ strand associates laterally and tightly with a TJ strand on an opposing membrane of an adjacent cell to form a paired strand [3,4].

* *Corresponding author*. Tel.: +81 6 6879 8176; fax: +81 6 6879 8199.
E-mail address: masuo@phs.osaka-u.ac.jp (M. Kondoh).

[1] These authors contributed equally to this work.

Abbreviations: C-CPE, the C-terminal fragment of *Clostridium perfringens* enterotoxin; PSIF, protein synthesis inhibitory factor; TJ, tight junction; CPE, *Clostridium perfringens* enterotoxin; TER, transepithelial electric resistance; C-CPE-PSIF, C-CPE fused to PSIF; PCR, polymerase chain reaction; LDH, lactate dehydrogenase; FD-4, fluorescein-isothiocyanate-dextran with a molecular weight of 4000

0006-2952/$ – see front matter
doi:10.1016/j.bcp.2006.10.002

Recent studies have revealed the molecular architecture of TJ strands and shown that TJs consist of three types of integral membrane proteins: occludin, junctional adhesion molecule, and claudins [5,6]. Occludin, an ~65 kDa integral membrane protein with four transmembrane domains, was the first component identified in TJ strands [7]; however, gene knockout analysis proved that it is not essential for forming TJ strands [8]. Junctional adhesion molecule has a single transmembrane domain and associate laterally with TJ strands, but it does not form TJ strands [9]. Thus, occludin and junctional adhesion molecule are not thought to be essential for the structure or function of TJs; however, claudin, an ~24 kDa integral membrane protein with four transmembrane domains, is thought to be essential for TJs. Overexpression of claudin in mouse L fibroblasts causes the formation of TJ strands and a TJ barrier [10,11]. In addition, claudin-based TJs have been shown to be directly involved in intercellular sealing [12–14].

There are more than 20 members of the claudin family, and the expression profiles and barrier function of each member differs by tissue [5,15]. For example, mice deficient in claudin-1 and -5 lose the barrier function of the epidermis and the blood-brain-barrier, respectively [16,17]. Each isoform of claudin can form homopolymers as well as heteropolymers with the other claudins, and each polymer laterally associates between adjacent cells [18]. One report proposed that the tightness of paired TJ strands is determined by the number and type of species of claudins and their mixing ratio in strands [5,18]. Thus, claudin family members are responsible for the barrier function of TJs, that is, the regulation of paracellular movement of water and solutes across epithelia [19]. A method to modulate the barrier function of claudins could therefore be a promising tool for understanding claudin function and for enhancing drug delivery.

Clostridium perfringens enterotoxin (CPE) is the substance that causes the symptoms of *C. perfringens* food poisoning in man [20]. The N-terminal half of CPE is responsible for toxicity, and the C-terminal half (C-CPE) plays a role in cell binding [20]. Interestingly, the CPE receptor is identical to claudin-4, and C-CPE has been shown to modulate the TJ barrier by binding to claudin-4 on the cell surface [12,21]. Furthermore, treatment of cells with C-CPE reduces claudin-4 levels in TJs, resulting in a disruption of the TJ barrier function [12]. To our knowledge, C-CPE is the only known modulator of claudin.

Based on this information, we suspected that we could create a claudin modulator using C-CPE as a prototype. Therefore, we previously identified the region of C-CPE necessary for modulating the TJ barrier and for binding to claudin-4. Deletion analysis revealed that the C-terminal 16 amino acids of C-CPE participate in modulation of the TJ barrier by C-CPE and for interaction between C-CPE and claudin-4 [22,23]. Previously, substitution of Tyr310 with Cys reduced binding of CPE to the brush border membrane in rabbits [24]. In the current study, we investigated roles of the tyrosines (Tyr306, Tyr310 and Tyr312) of C-CPE in claudin-4 binding and modulation of the TJ barrier. We also examined the effects of double and triple mutants of Tyr306, Tyr310, and Tyr312.

2. Materials and methods

2.1. Materials

Anti-His-tag and anti-claudin-4 antibodies were obtained from Novagen (Madison, WI) and Zymed Laboratories (South San Francisco, CA), respectively. Ni-resin was purchased from Invitrogen (Carlsbad, CA).

2.2. Cell cultures

Caco-2 human intestinal cells were cultured in Dulbecco's modified Eagle's medium containing 10% fetal bovine serum in a 5% CO_2 atmosphere at 37 °C. Caco-2 cells (passages 65–72) were used for experiments. Claudin-4-expressing mouse fibroblast L cells (CL4/L cells) were kindly provided by Tsukita and Furuse [12,15] and were maintained in modified Eagle's medium containing 10% fetal bovine serum at 37 °C.

2.3. Preparation of mutant C-CPE

The indicated residues were mutated to Ala by polymerase chain reaction (PCR) using a forward primer containing *Nde*I site, a reverse primer containing a *Bam*HI site, and pET16b-His_{10}C-CPE as a template [23]. The primer sequences are listed in Table 1. The resulting PCR products were ligated with *Nde*I/*Bam*HI-digested pET16b vector (Novagen), and the DNA sequence was confirmed. Each plasmid was transduced into *Escherichia coli* BL21 (DE3), and production of mutant C-CPEs were induced by addition of isopropyl-β-D-thiogalactopyranoside. The cells were harvested and lysed in buffer A (10 mM Tris–HCl, pH 8.0, 400 mM NaCl, 5 mM $MgCl_2$, 10% glycerol, 0.1 mM *p*-amidinophenyl methanesulfonyl fluoride hydrochloride, and 1 mM β-mercaptoethanol) containing 8 M urea. The lysates were applied onto a Ni-NTA column, and mutant C-CPEs were eluted with buffer A containing 100–1000 mM imidazole. The buffer was exchanged with phosphate-buffered saline using C-CPE as a claudin modulator by gel filtration using a PD-10 column (GE Healthcare Bio-Sciences Co., Piscataway, NJ). The concentrations of mutant C-CPEs were estimated using a protein assay kit with bovine serum albumin as a standard (Bio-Rad, Hercules, CA). The purification of mutant C-CPEs was confirmed by sodium dodecyl sulfate-polyacrylamide gel electrophoresis (SDS-PAGE), followed by staining of the gels with Coomassie Brilliant Blue (data not shown).

2.4. Preparation of mutant C-CPE-PSIF

Plasmids expressing mutant C-CPEs fused to protein synthesis inhibitory factor (PSIF) were prepared as described below. Mutant C-CPE fragments were amplified by PCR using primers 5′-catgccatggccgaaagatgtgttttaacagttcc-3′ (forward; *Nco*I site underlined) and 5′-atagtttagcggccgcaaatttttgaaataatattgaataagg-3′ (reverse; *Not*I site underlined) and with pET16b plasmids encoding each mutant C-CPE as templates. The *Nco*I/*Not*I-digested mutant C-CPE fragments were inserted into *Nco*I/*Not*I-digested pY02-C-CPE-PSIF to generate pY02 mutant C-CPE-PSIF plasmids [25]. The sequence of the plasmids was confirmed. The C-CPE-PSIF and mutant C-CPE-PSIF plasmids

Table 1 – Primers used for site-directed mutagenesis

Primers	Sequences (5′–3′)
Common forward primer	ggaattc cat atg gaa aga tgt gtt tta aca gtt cca tct aca
Reverse primer for Y306A	cgggatcc tta aaa ttt ttg aaa taa tat tga ata agg gta att tcc act *agc* tga tga att agc ttt cat tac
Reverse primer for Y310A	cgggatcc tta aaa ttt ttg aaa taa tat tga ata agg *agc* att tcc act ata tga tga att agc ttt c
Reverse primer for Y312A	cgggatcc tta aaa ttt ttg aaa taa tat tga *agc* agg gta att tcc act ata tga
Reverse primer for Y306A/Y310A	cgggatcc tta aaa ttt ttg aaa taa tat tga ata agg *agc* att tcc act *agc* tga tga att agc ttt cat tac
Reverse primer for Y306A/Y312A	cgggatcc tta aaa ttt ttg aaa taa tat tga *agc* agg gta att tcc act *agc* tga tga att agc ttt cat tac aag
Reverse primer for Y310A/Y312A	cgggatcc tta aaa ttt ttg aaa taa tat tga *agc* agg *agc* att tcc act ata tga tga att agc ttt cat tac
Reverse primer for Y306A/Y310A/Y312A	cgggatcc tta aaa ttt ttg aaa taa tat tga *agc* agg *agc* att tcc act *agc* tga tga att agc ttt cat tac

The underline in forward primer and in reverse primer is *Nde*I site and *Bam*HI site, respectively. The italic letters in the reverse primer indicated the site of mutation.

were transduced into *E. coli* strain TG1. The cells were grown at 37 °C in 2YT medium containing 2% glucose to a density at 600 nm of 0.6–0.9, and the medium was changed to 2YT medium containing 1 mM isopropyl-β-D-thiogalactopyranoside. After an additional 18 h of culture at 30 °C, the conditioned medium was recovered. The medium was applied to anti-FLAG M2 affinity gel, and the proteins bound to the gel were eluted with FLAG peptide. The buffer was changed to phosphate-buffered saline (PBS) using a PD-10 column (GE Healthcare Bio-Sciences Co., Piscataway, NJ). Purification of mutant C-CPE-PSIF was confirmed by sodium dodecyl sulfate-polyacrylamide gel electrophoresis (SDS-PAGE), followed by staining with Coomassie Brilliant Blue and by immunoblotting with anti-FLAG M2 antibody (data not shown). Protein levels were measured using a commercially available assay kit with bovine serum albumin as a standard (Bio-Rad, Hercules, CA).

2.5. Assay of cytotoxicity

The cytotoxicity of C-CPE-PSIF and mutant C-CPE-PSIF proteins was evaluated by measuring the release of lactate dehydrogenase (LDH) from cells. CL4/L cells were treated with C-CPE or mutant C-CPE-PSIF proteins at the indicated concentrations for 36 h. LDH release was then measured using a CytoTox96 Non Radioactive Cytotoxicity Assay kit according to the manufacturer's protocol (Promega).

2.6. Competition analysis

CL4/L cells were pretreated with C-CPE or mutant C-CPE at the indicated concentrations for 1 h, after which C-CPE-PSIF was added to the cells. After an additional 36 h of culture, LDH release was assayed as described above.

2.7. Pull-down assay

Confluent Caco-2 cells were harvested and lysed in lysis buffer (1% Triton X-100, 0.2% sodium dodecyl sulfate, 150 mM NaCl, 10 mM HEPES [pH 7.4], 2 mM EDTA, and 1% protease inhibitor cocktail [Sigma, St Louis, MO]). C-CPE or mutant C-CPEs were incubated with the lysates for 30 min at 37 °C and then mixed with Ni-resin beads (Invitrogen, Gaithersburg, MD). After an additional 2 h at 4 °C, the beads were washed with lysis buffer, and bound proteins were analyzed by SDS-PAGE followed by Western blotting using anti-human claudin-4 (Zymed Laboratories, San Francisco, CA) and anti-His-tag antibodies (Novagen). The bound primary antibody was detected with a peroxidase-labeled secondary antibody followed by visualization with chemiluminescence reagents (Amersham Bioscience, NJ).

2.8. Transepithelial resistance (TER) assay

Caco-2 cells were seeded in Transwell chambers (Nunc, Roskilde, Denmark) at a subconfluent density. The formation of TJ barriers in Caco-2 monolayers was monitored by measuring the TER using a Millicell-ERS epithelial volt-ohmmeter (Millipore Co). When the TER values reached a plateau for continuous 3 days, the Caco-2 monolayers were treated with C-CPE or mutant C-CPEs on the apical side of the chamber, and the TER values were measured. The TER values were normalized by the area of the Caco-2 monolayer. The TER value of a blank Transwell chamber (background) was subtracted from the TER of cell monolayers.

2.9. In situ loop assay

Wistar male rats (250–280 g) were obtained from Animal and Material Laboratories Inc. (Tokyo, Japan). The rats were maintained in an environmentally controlled room (23 ± 1.5 °C) with a 12 h light/12 h dark cycle and allowed access to standard rodent chow and water *ad libitum*. The rats were allowed a week to adapt. The experimental protocol for the *in situ* loop assay was approved by the ethics committee of Showa Pharmaceutical University. Intestinal absorption of fluorescein-isothiocyanate-dextran with a molecular weight of 4000 (FD-4) was investigated by *in situ* loop assay as follows. Rats were anesthetized with thiamylal sodium (Mitsubishi Pharma Co. Ltd., Osaka, Japan). A midline abdominal incision was made, and the lumen of the jejunum was washed with saline. A jejunal loop (5 cm in length) was prepared by closing both ends with sutures. A mixture of FD-4 and C-CPEs in 200 μl

of PBS was administered into the jejunal loop. Blood was collected from the jugular vein at the indicated time points. The plasma concentration of FD-4 was determined with a fluorescence spectrophotometer (Fluoroskan Ascent FL; Thermo Electron Corp., Waltham, MA). The area under the plasma concentration–time curve from 0 to 4 h (AUC_{0-4}) was calculated by the trapezoidal method.

3. Results

3.1. *Roles of Tyr306, Tyr310 and Tyr312 in the interaction between C-CPE and claudin-4*

We previously found that the C-terminal 16 amino acids are responsible for ability of C-CPE to modulate the TJ barrier and to bind to claudin-4 [22,23] (Fig. 1). Kokai-Kun et al. showed that substitution of Tyr310 with Cys reduced binding of CPE to the brush border membrane in rabbits [24]. Here, we focused on three tyrosine residues in this region, namely Tyr306, Tyr310 and Tyr312. To evaluate the function of these tyrosine residues, we generated Tyr306, Y310A and Y312A mutants by site-directed mutagenesis. We then examined the ability of these mutants to inhibit the toxicity of C-CPE-PSIF, a molecule that specifically targets and is toxic to claudin-4-expressing cells [25]. In CL4/L cells, pretreatment with C-CPE attenuated toxicity of C-CPE-PSIF in a dose-dependent manner (Fig. 2A). The Y306A, Y310A and Y312A mutants had reduced abilities to inhibit C-CPE-PSIF-induced cytotoxicity. We also used a pull-down assay to examine the ability of these mutants to interact with claudin-4 in Caco-2 lysates, which have well-developed TJs [22]. Less claudin-4 precipitated with the Y306A and Y310A mutant than with C-CPE, but the Y312A mutant bound claudin-4 as effectively as C-CPE (Fig. 2B). The extra band below claudin-4 was observed in C-CPE, mutants and C-CPE/mutants-treated samples. The extra band was due to non-specific reaction of anti-claudin-4 Ab with histidine-tag (data not shown).

3.2. *Interaction of double mutants of C-CPE with claudin-4*

To evaluate the synergistic effects of Tyr306, Tyr310, and Tyr312 on the ability of C-CPE to interact with claudin-4, we generated double tyrosine to alanine substitution mutants (Y306A/Y310A, Y306A/Y312A, and Y310A/Y312A). As shown in Fig. 3A, we investigated the interaction of double mutants with claudin-4 in the C-CPE-PSIF competitive assay. Pretreatment of cells with C-CPE at 10 μg/ml inhibited LDH release to 18% of the vehicle-treated group, whereas treatment of cells with the Y306A/Y310A and Y306A/Y312A mutants did not affect C-CPE-PSIF-induced LDH release even at 10 μg/ml. Treatment of cells with Y310A/Y312A at 10 μg/ml partially attenuated the cytotoxicity of C-CPE-PSIF. A pull-down assay revealed that the Y306A/Y310A and Y306A/Y312A mutants completely lost the ability to bind claudin-4. Y310A/Y312A mutant had the partly reduced ability to bind claudin-4 (Fig. 3B). Thus, mutation of Tyr310 and Tyr312 to alanine reduced precipitation of claudin-4 in the pull down assay.

3.3. *Effects of double mutants on TJ barrier function in Caco-2 cells*

Next, we investigated the effects of the mutants on the TJ barrier function in Caco-2 monolayers grown in Transwells. Treatment of the cells with C-CPE, the Y310A and Y312A mutant for 18 h reduced the TER value, a marker of tightness in the TJs, from 295 to 30 and from 326 to 49 Ω cm^2, respectively (Fig. 4A). The Y306A and Y310A/Y312A mutants caused less of a reduction in TJ barrier function than C-CPE. The Y306A/Y310A and Y306A/Y312A mutants, however, had almost no effect on the TJ barrier function (from 291 to 261 and from 289 to 254 Ω cm^2, respectively; Fig. 4A).

We previously found that C-CPE enhances rat jejunal absorption of FD-4 by interacting with claudin-4 [23]. We further evaluated the ability of each mutant to enhance jejunal absorption of FD-4 (Fig. 4B and C). We found that the Y310A mutant enhanced absorption to a similar extent as C-CPE,

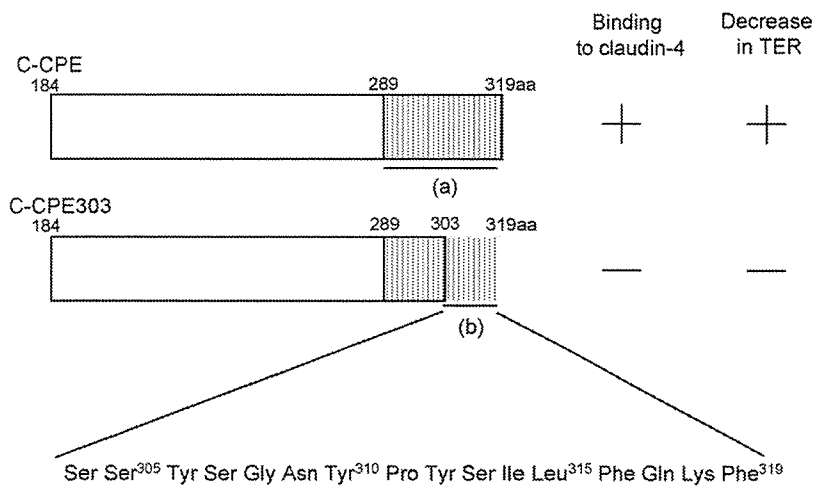

Fig. 1 – Diagram of C-CPE structure. C-CPE is the C-terminal fragment of CPE [21]. C-CPE binds to claudin-4 and decreases TJ barrier function as indicated by a decrease in TER [12]. The C-terminal 30 amino acids of CPE and C-CPE mediate interaction with the CPE receptor and claudin, respectively (a) [22,23,32]. Further analysis shows that the C-terminal 16 amino acids are responsible for the interaction of C-CPE with claudin and for its ability to decrease the TJ barrier function (b) [22,23].

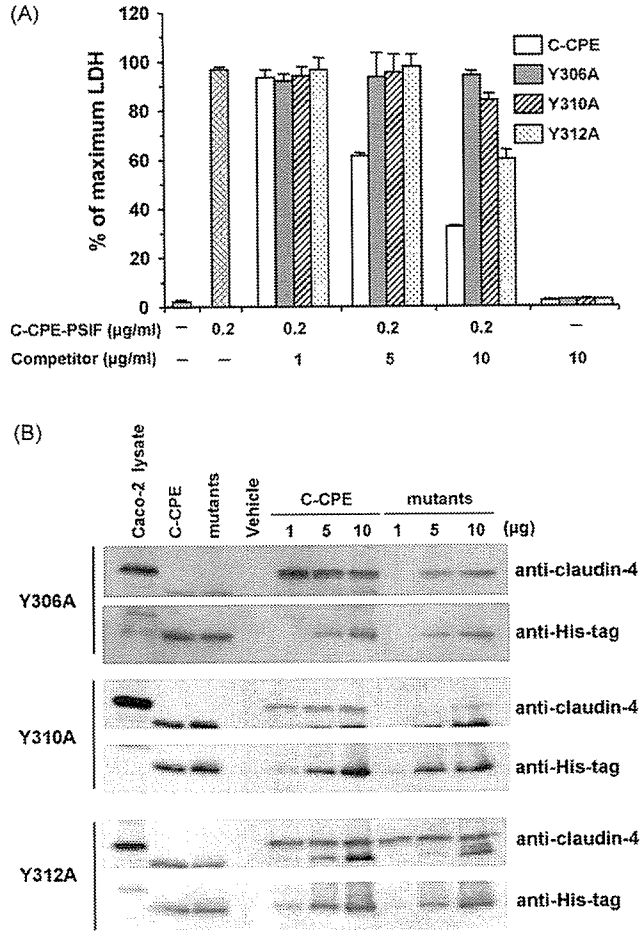

Fig. 2 – Effects of Tyr306, Tyr310 and Tyr312 on the interaction of C-CPE with claudin-4. (A) Competitive inhibition of C-CPE-PSIF-induced cytotoxicity by mutants of C-CPE. Claudin-4-expressing L (CL4/L) cells were pretreated with the indicated concentrations of C-CPE or C-CPE mutants for 1 h. The cells were then incubated with 0.2 μg/ml of C-CPE-PSIF. After 36 h, LDH release was assessed using a commercially available kit. The results are representative of three independent experiments, and the values are means ± S.D. ($n = 3$). (B) Pull-down assay. Confluent Caco-2 cells were harvested and lysed in lysis buffer. The lysate (10 μg) was incubated with vehicle, C-CPE, or mutants of C-CPE for 30 min at 37 °C. After addition of Ni-resin, the lysate was incubated for 3 h at 4 °C. The resin was then precipitated, and the bound proteins were analyzed by SDS-PAGE followed by Western blotting using anti-claudin-4 or anti-His-tag antibodies. The lanes containing Caco-2 lysates (10 μg), C-CPE (1 μg), and mutants of C-CPE (1 μg) were positive controls for claudin-4, C-CPE, and mutants of C-CPE, respectively. The results are representative of three independent experiments.

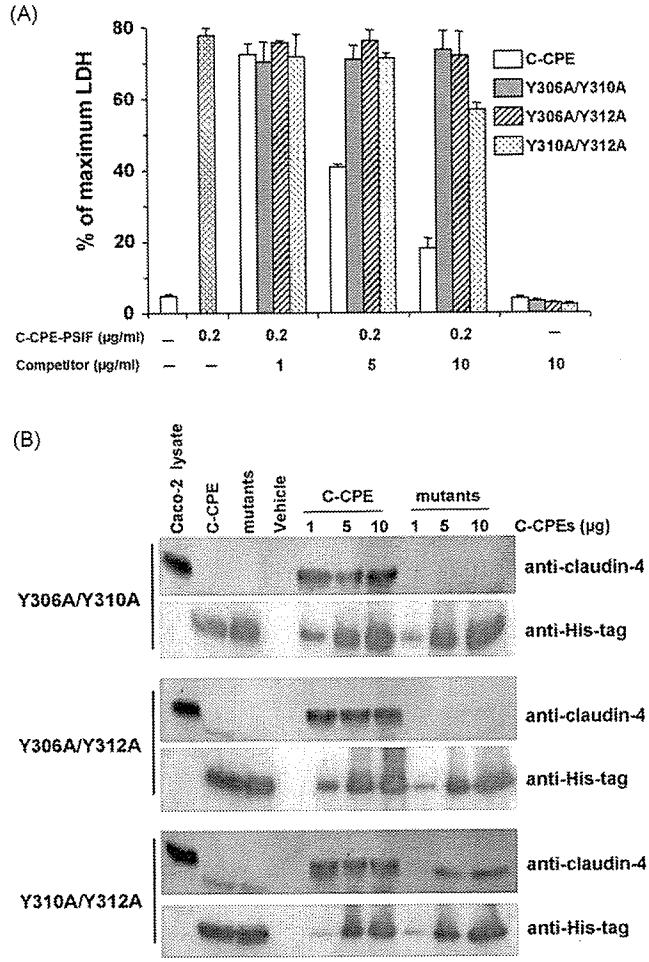

Fig. 3 – Interaction of double mutants at residues 306, 310, and 312 of C-CPE with claudin-4. (A) Competition assay. CL4/L cells were incubated with double mutants at the indicated concentration for 1 h and then mixed with C-CPE-PSIF (0.2 μg/ml). After 36 h, LDH release was assessed using a commercially available kit. The results are representative of three independent experiments. Values are means ± S.D. ($n = 3$). (B) Pull-down assay. Caco-2 lysates (10 μg) were incubated with double mutants (Y306A/Y310A, Y306A/Y312A, or Y310A/Y312A) for 30 min at 37 °C. Ni-resin was then added, and the lysate was incubated for 3 h at 4 °C. Next, the resin was precipitated, and the bound proteins were analyzed by SDS-PAGE followed by Western blotting.

whereas the Y312A and Y306A mutants had weaker abilities to enhance absorption ($AUC_{0-4\,h} = 2.0$ and 6.4, respectively). Double mutant Y306A/Y310A had a moderate absorption-enhancing activity, similar to the Y306A mutant. In contrast, the Y306A/Y312A and Y310A/Y312A double mutants lost the ability to enhance absorption. Thus, there are some differences between the effects of some of the mutants on the TER values and jejunal absorption.

3.4. *Effects of triple mutant Y306A/Y310A/Y312A on the ability to bind to claudin-4 and to modulate the TJ barrier function*

Finally, to clarify role of tyrosine residues 306, 310, and 312 in C-CPE function, we mutated all three to alanine, generating the Y306A/Y310A/Y312A triple mutant. To evaluate the

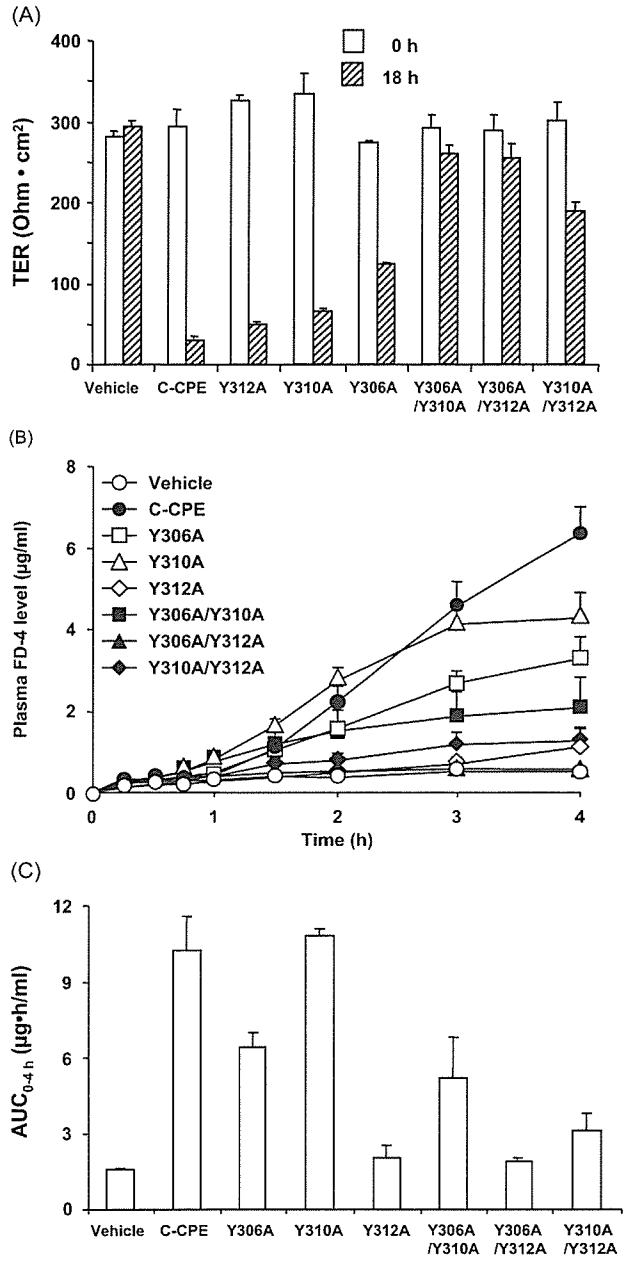

Fig. 4 – Effects of mutants of C-CPE on the TJ barrier function and jejunal absorption. (A) Effects of mutants on the TJ barrier function of Caco-2 monolayer cells. Confluent Caco-2 cells were cultured in Transwell chambers for 10–14 days. When TER values stabilized, C-CPEs were added to the basal side of the Transwell chamber at the indicated concentrations. TER values were measured after 0 and 18 h. Values are means ± S.D. (n = 4). The results are representative of three independent experiments. (B) Effects of mutants on jejunal absorption of FD-4 in rat. Rat jejunum was treated with FD-4 (10 mg/ml) in the presence of vehicle, C-CPE (0.2 mg/ml), or mutant C-CPEs (0.2 mg/ml). The FD-4 levels in plasma collected from the jugular artery were determined at the indicated times. Values are means ± S.E.M. (n = 4). (C) The $AUC_{0-4\ h}$ values were calculated from (B) and are means ± S.E.M. (n = 4). The results shown in (B) and (C) are representative of three independent experiments.

interaction of Y306A/Y310A/Y312A mutant with claudin-4, we performed a competitive assay using C-CPE-PSIF (Fig. 5A) and a pull-down assay using Caco-2 lysates (Fig. 5B). As indicated in Fig. 5A and B, the triple mutant lost the ability to interact with claudin-4. Furthermore, Fig. 5C–E shows that the triple mutant could not modulate TJ barrier function or enhance jejunal absorption.

4. Discussion

Claudins are critical for the barrier function of TJs in epithelia and endothelia [5]. This suggests that modulating the barrier function of claudins can be employed to deliver drugs, and we and Tsukita and colleagues have indeed shown that claudin is a promising target for the development of a drug delivery system [16,17,23,25]. Methods of modulating the barrier function of claudins are, however, very limited, and to our knowledge C-CPE is the only known modulator of a claudin (claudin-4) in TJs [12]. Therefore, we have sought to develop claudin modulators using C-CPE prototype and identified the part of C-CPE that modulates the TJ barrier function [22]. In the current study, we used site-directed mutagenesis and functional assays to clarify the roles of tyrosines 306, 310, and 312 of C-CPE. We found that these three tyrosine residues are critical for binding of C-CPE to claudin-4 and for modulation of the TJ barrier function.

Interestingly, the Y312A mutant had different effects in the pull-down assay using Caco-2 lysates than in the competitive assay using C-CPE-PSIF. Specifically, the Y312A mutant bound to claudin-4 in the pull down assay but it displayed reduced binding in the C-CPE-PSIF competitive assay. These conflicting results could be due to differences in the assay systems or the species of claudin-4: the former assay investigates the interaction of C-CPE with human claudin-4 in cell lysates, whereas the latter assesses the interaction with mouse claudin-4 on the cell membrane [25]. Claudin is tetra-transmembrane protein with two extracellular loop domains [5], and CPE and C-CPE interact with the second of these extracellular loops [22,26]. Examination of the amino acid sequence in the second extracellular loop domain of claudin-4 (EC2cld4) reveals, in fact, that they are different in mouse (GenBank accession no. AF087822; residues 145–163; RDFYNPMVASGQKREMGAS; underline indicates sequence differences with human claudin-4) and human (GenBank accession no. BC000671; residues 142–160; NIIQDFYNPI-VASGQKREM; underline indicates sequence differences with mouse claudin-4) [15].

The Y312A mutant also had different effects between TER assay and *in situ* loop assay. Although the Y312A mutant reduced TER values in Caco-2 monolayer cells, the Y312A mutant did not enhance rat jejunal absorption of FD-4. TER is a marker of tightness in the TJs, but we did not evaluate the permeability of FD-4 in Caco-2 monolayer cells. Several reports indicate that TER values did not reflect permeability of non-electrolytes [27,28]. Therefore, decrease in TER values may be inconsistent with influx of paracellular markers in Caco-2 cells. The amino acids sequences in EC2cld4 are also different in rat (GenBank accession no. NM_001012022; residues 145–163; RDFYNPIVASGQKREMGAS; underline indicates sequence

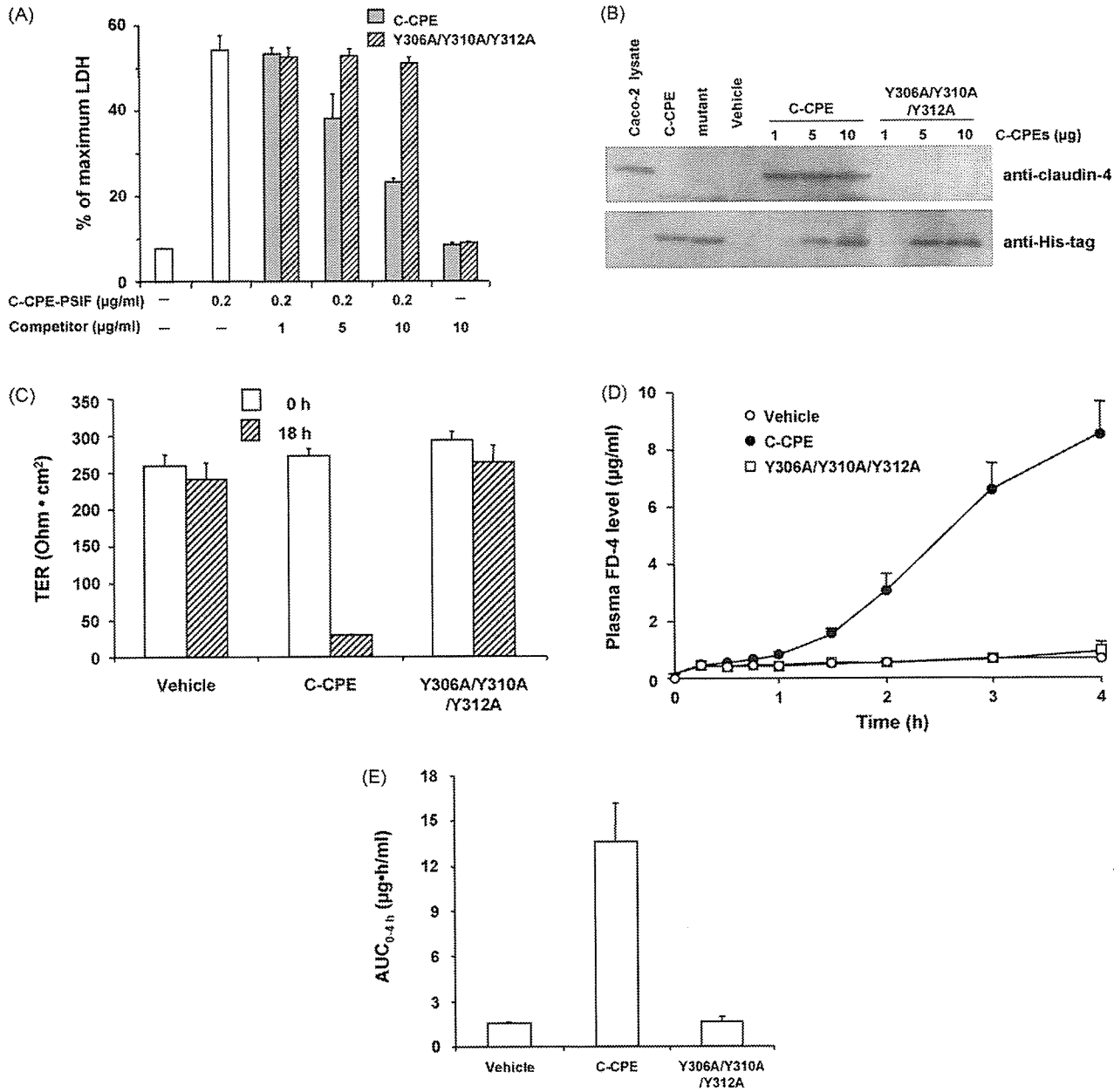

Fig. 5 – Effect of triple mutation on the activities of C-CPE. Interaction of the triple mutant with claudin-4 was examined using competitive assay with C-CPE-PSIF (A) and a pull-down assay (B) as described in Fig. 2A and B, respectively. Effects of the triple mutant on the TJ barrier in Caco-2 monolayer cells (C) and jejunal absorption in rat (D and E) were assayed as described in Fig. 4. The values in (B) and (C) are means ± S.D. (n = 4), and those in (D) and (E) are means ± S.E.M. (n = 4). The results are representative of three independent experiments.

differences with human claudin-4) and human (GenBank accession no. BC000671; residues 142–160; NIIQDFYNPIVASGQKREM; underline indicates sequence differences with rat claudin-4) [15]. The differences of EC2cld4 between rat and human may contribute the contradiction of data on Y312A in TER assay and *in situ* loop assay.

We also found that mutation of Tyr310 to alanine reduced binding of C-CPE to claudin-4. This finding agrees with a previous report by Kokai-Kun et al. showing that replacement of Tyr310 with cysteine reduced the ability of CPE to bind to its receptor [24]. Tyr310 may participate in interaction of C-CPE with claudin-4 because the Y310A mutant had the ability to modulate the TJ barrier function in Caco-2 monolayers and to enhance rat jejunal absorption. Whether claudin-4 binding and modulation of the TJ barrier function can be separated is a critical question for the design of future claudin modulators. Mutation of Tyr306 to alanine reduced both activities suggested that they are mediated by the same functional domain on C-CPE. Results with the Y310A mutant, however, indicate that different residues mediate these two functions. In fact, the Y312A mutant did not enhance jejunal absorption in rats (Fig. 4B and C), although it bound claudin-4